

AD-A081 807

CASE WESTERN RESERVE UNIV CLEVELAND OHIO ULTRASONICS --ETC F/6 8/10
ACOUSTIC STUDIES OF COLLOIDAL SUSPENSIONS AND MARINE SEDIMENTS.--ETC(U)
JAN 80 M A BARRETT-GUELTEPE, M E GUELTEPE N00014-75-C-0557

UNCLASSIFIED

TR-46

NL

1
AL
4/8/80

END
DATE
FILMED
4-80
DTIC

ADA 081 807

12

OFFICE OF NAVAL RESEARCH

Contract N00014-75-C-0557

Project NR 384-305

IVEL #

9

TECHNICAL REPORT NO. 46

14

TR-46

6

ACOUSTIC STUDIES OF COLLOIDAL SUSPENSIONS AND MARINE SEDIMENTS.
I. THEORETICAL CONSIDERATIONS AND HIGH FREQUENCY MEASUREMENTS.

by

M. A. Barrett-Gültepe, M. E. Gültepe and E. B. Yeager

12/61

Ultrasonic Research Laboratory

and

Case Laboratories for Electrochemical Studies

Case Institute of Technology

Case Western Reserve University

Cleveland, Ohio 44106

11/ 15 Jan 1980

SDTIC ELECTE D
MAR 12 1980
A

Reproduction in whole or in part is permitted for any
purpose of the United States Government

DDC FILE COPY

403881

80 3 11 010

Unclassified

SECURITY CLASSIFICATION OF THIS PAGE (When Data Entered)

REPORT DOCUMENTATION PAGE		READ INSTRUCTIONS BEFORE COMPLETING FORM
1. REPORT NUMBER 46	2. GOVT ACCESSION NO.	3. RECIPIENT'S CATALOG NUMBER
4. TITLE (and Subtitle) ACOUSTIC STUDIES OF COLLOIDAL SUSPENSIONS AND MARINE SEDIMENTS. I. THEORETICAL CONSIDERATIONS AND HIGH FREQUENCY MEASUREMENTS		5. TYPE OF REPORT & PERIOD COVERED Technical Report
		6. PERFORMING ORG. REPORT NUMBER
7. AUTHOR(s) M. A. Barrett-Gultepe, M.E. Gultepe, and E. B. Yeager		8. CONTRACT OR GRANT NUMBER(s) N00014-75-C-0557
9. PERFORMING ORGANIZATION NAME AND ADDRESS Ultrasonic Research Laboratory Case Western Reserve University Cleveland, Ohio 44106		10. PROGRAM ELEMENT, PROJECT, TASK AREA & WORK UNIT NUMBERS NR384-305
11. CONTROLLING OFFICE NAME AND ADDRESS Office of Naval Research Physics Section -Code 421 Arlington, Virginia 22217		12. REPORT DATE 15 January 1980
		13. NUMBER OF PAGES 63
14. MONITORING AGENCY NAME & ADDRESS (if different from Controlling Office)		15. SECURITY CLASS. (of this report) Unclassified
		15a. DECLASSIFICATION/DOWNGRADING SCHEDULE
16. DISTRIBUTION STATEMENT (of this Report) Approved for public release; distribution unlimited		
17. DISTRIBUTION STATEMENT (of the abstract entered in Block 20, if different from Report)		
18. SUPPLEMENTARY NOTES		
19. KEY WORDS (Continue on reverse side if necessary and identify by block number) acoustic absorption, velocity, sediments, colloids, interfacial phenomena		
20. ABSTRACT (Continue on reverse side if necessary and identify by block number) The propagation of sound in concentrated colloidal dispersions and marine sediments has been theoretically examined with particular attention to the influence of the interfacial phenomena. In addition to the heretofore identified factors which may affect the propagation of sound in sediments, a possible new effect, heterodefloculation of various mineral grains, was experimentally demonstrated. The contribution of the interparticle forces to the acoustic particles in sediments is discussed. The treatment of absorption and velocity with the interparticle forces taken into account using the D.L.V.O. theory do not lead to		

DD FORM 1473
1 JAN 73

EDITION OF 1 NOV 65 IS OBSOLETE

S/N 0102-LF-014-6601

Unclassified

SECURITY CLASSIFICATION OF THIS PAGE (When Data Entered)

Unclassified

SECURITY CLASSIFICATION OF THIS PAGE (When Data Entered)

Continued (Block #20)

of such forces in a simple geometry of particles, although the assumption of small flocs increases the estimated influence considerably.

S/N 0102-LF-014-6601

Unclassified

SECURITY CLASSIFICATION OF THIS PAGE (When Data Entered)

TABLE OF CONTENTS

	Page
Title Page	i
Document Control Data	ii
List of Figures	v
List of Tables	vi
I. Objectives of Work	1
II. Background	1
A. Heterodeflocculation	5
B. Adsorption of organics on clay	7
C. Interparticle forces	8
III. The Theory of the Interparticle Forces in Marine Colloids and Sediments	9
IV. The Theory of the Attenuation and Velocity of Sound Waves in Concentrated Colloidal Dispersions and Sediments	16
A. Velocity	22
B. McCann's treatment	26
C. Present treatment	28
V. Experimental	30
A. Montmorillonite	30
B. Kaolin	31
C. Velocity and attenuation measurements	34
VI. Discussion and Results	37
Key to Symbols	54
References	56
Distribution List	60

Accession for	
NTIS GRA&I	<input checked="" type="checkbox"/>
DDC TAB	<input type="checkbox"/>
Unannounced	<input type="checkbox"/>
Justification	
By	
Distribution/	
Availability Codes	

LIST OF FIGURES

	page
1a. Diagrammatic sketch of the two-layer structure	4
1b. Diagrammatic sketch of the three layer structure	4
2. Possible configurations of kaolin particles	6
3. Total potential energy of interaction between two particles as a function of separation	10
4. Potential diagram of the interaction of two diffuse double layers as a function of κH	12
5. Calculated absorption values for kaolin dispersions in water at 1 MHz at 25°C	23
6. The vibrations of a line of charged particles	26
7. Particle size distribution of the kaolin sample used in the present work	33
8. Velocity ratio measured for a 10% by volume kaolin suspension with increasing amounts of montmorillonite	38
9. Acoustic absorption values for kaolin suspensions at 1 MHz	39
10. Acoustic absorption values for kaolin suspensions at 5 MHz	40
11. Velocity of sound in kaolin dispersions at 2 MHz	41
12. The Y values for eq. (42) found to bring calculated values of acoustic absorption and velocity into agreement with experimental values at 1 and 2 MHz	45
13. Experimental and calculated values of acoustic absorption of kaolin suspensions at 1 and 5 MHz,	46
14. The Y values calculated as a function of volume % using DLVO theory in a configuration of parallel plates in domains that fill half the volume	48
15. Ratio of velocity of sound in polystyrene latex suspensions, c , to that in water, c_0 at 2 MHz	51
16. Possible model for heterodeflocculation of kaolin platelets around neutral pH by specific adsorption of the negatively charged montmorillonite particles on the positively charged edges of kaolin.	53

LIST OF TABLES

		page
TABLE I	Batch III, No-Chemical Refined Clay	32
TABLE II	Calculated Values of Force Constant f and Y for Various Volume Fractions ϕ , and Particle Thickness 550\AA	47

I. OBJECTIVES OF WORK

The aim of the present work is to examine theoretically and experimentally the various possible factors and effects which control the acoustic absorption and velocity in colloidal suspensions and sediments. The acoustic measurements are being carried out over a wide range of frequencies extending well into the audio. The results reported herein are at MHz frequencies. However, low frequency measurements will be carried out in the near future.

In order to gain further insight into the factors influencing velocity and absorption in colloidal suspensions, some measurements have also been carried out on latex suspensions in which the particles have densities much closer to that of water. The major effort, however, is centered on studies involving clay.

II. BACKGROUND

Propagation of sound waves in the ocean, particularly shallow water bodies, is governed by losses in the suspended matter and sediments as well as intrinsic losses in sea water. The physical chemistry of the sediments and the suspended matter are very much influenced by the sea water.

The sediments on the sea floor,* consisting mainly of coarse

*Annually many millions of tons of suspended and dissolved matter are washed down by the rivers to the sea. In addition to clay, silt and sand, there is also organic matter carried to the sea. The amount varies considerably with the river. It is calculated¹ that the Mississippi alone carries 136 million tons of dissolved matter and 340 million tons of suspended matter into the sea each year.

fractions of sand and clay, form two main layers: an unconsolidated sediment layer on top of a consolidated mass. The finer particles are in the form of colloidal suspensions and also may be adsorbed on the specific sites of the large particles. Organic molecules may also adsorb on particles.

A model for the sea floor taking the above factors into account is necessary for underwater acoustics and geological studies. The acoustic models usually take into account the following factors:²⁻⁵

- (i) porosity
- (ii) frame rigidity
- (iii) compressibilities of the individual grains
- (iv) pressure
- (v) temperature gradients

For colloidal size sediments McCann⁶ has considered inter-particle forces as pure Coulombic repulsion forces between charged mineral particles. As pointed out by Barrett-Gültepe et al.⁷, there are shortcomings of his treatment.

Frequently in the literature the particles of sediments falling into the size range 'below 1 μ are designated as clay particles, without

regard to their mineralogical nature and include, for example, fine quartz and sand particles as well as kaolin. Although the same particle size of sand and kaolin may not differ in porosity, the two materials behave entirely differently under the same chemical conditions. For example, sand particles are negatively charged and do not show heteropolar behavior as kaolin. Therefore, our approach requires differentiation between these.

A classification of clay materials has been developed based on the crystal structure as follows: X-ray diffraction analysis has shown that the principal building elements of clay minerals are the two-dimensional arrays of silicon-oxygen tetrahedra and two-dimensional arrays of aluminum or magnesium-oxygen-hydroxyl octahedra. These occur either as alternate layers forming the "two layer clays" (e.g. kaolin) or as three layers in which each octahedral layer has two tetrahedral layers associated with it (e.g. montmorillonite). These two types are illustrated in Figs. 1a and 1b respectively. There are commonly ionic substitutions in the natural forming minerals, and these generate the families of clays.

The following factors in addition to those taken into consideration in earlier work should be explored in an attempt to produce a more adequate model of the sediments: 1) heterodeflocculation of sediment mixtures and the effect of this on the frame rigidity, 2) adsorption of organics on clay-sea water interfaces, and 3) the effect of interparticle forces.

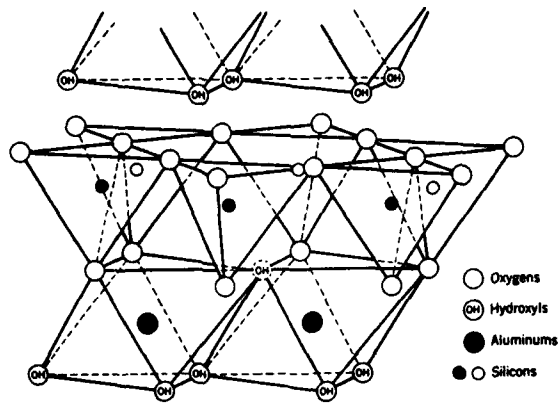


Fig. 1a. Diagrammatic sketch of the two layer structure.

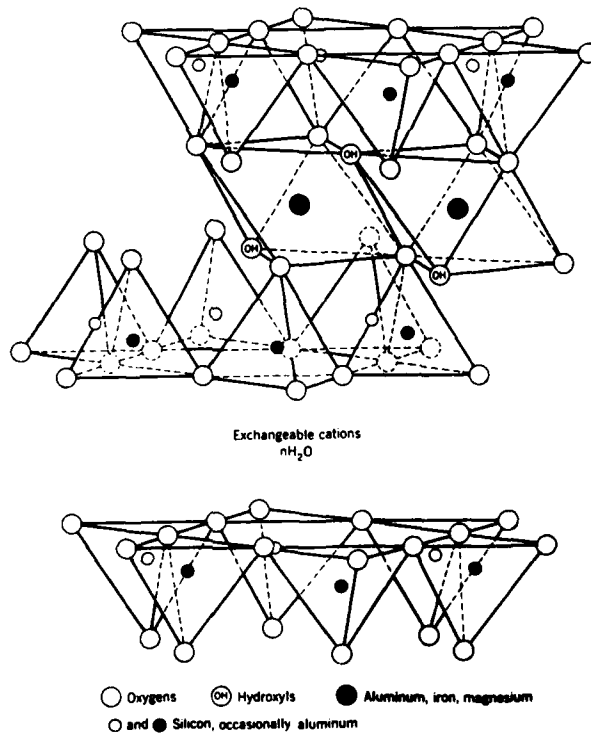


Fig. 1b. Diagrammatic sketch of the three layer structure.

A) Heterodeflocculation

It has been pointed out that clay particles such as kaolinites exhibit opposite charges on the faces (basal plane) and their edges:⁸ the faces are negatively charged and the edges positively charged at pH below 9. In the pH range found in the sea water, the clay particles show strong flocculation behavior. The positively charged edges interact with the negatively charged faces of the neighboring particles, thus forming the so-called cardhouse structure, Fig. 2. This type of behavior can be readily observed in dispersions of such particles around 10% by volume and up.

In the laboratory experiment, deflocculation of the system can be controlled by changing the pH or by the adsorption of surface active agents or of water soluble polymer. For example, progressively increasing pH produces progressively increasing negative charge. At one particular pH the kaolin crystal carries negative charge on all faces, and thus the system shows complete dispersion or in more conventional terms, shows complete deflocculation. Such deflocculation occurs at pH 9 to 10. Of course, in sea water it is unlikely that such variation of pH is encountered. However, adsorption of very small mineral grains, such as montmorillonite and illites on the positively charged edges of kaolin crystals will produce destruction of the cardhouse structure and complete heterodeflocculation* of kaolin particles will be achieved without

* Heterodeflocculation involves the deflocculation of systems with two or more types of particles.

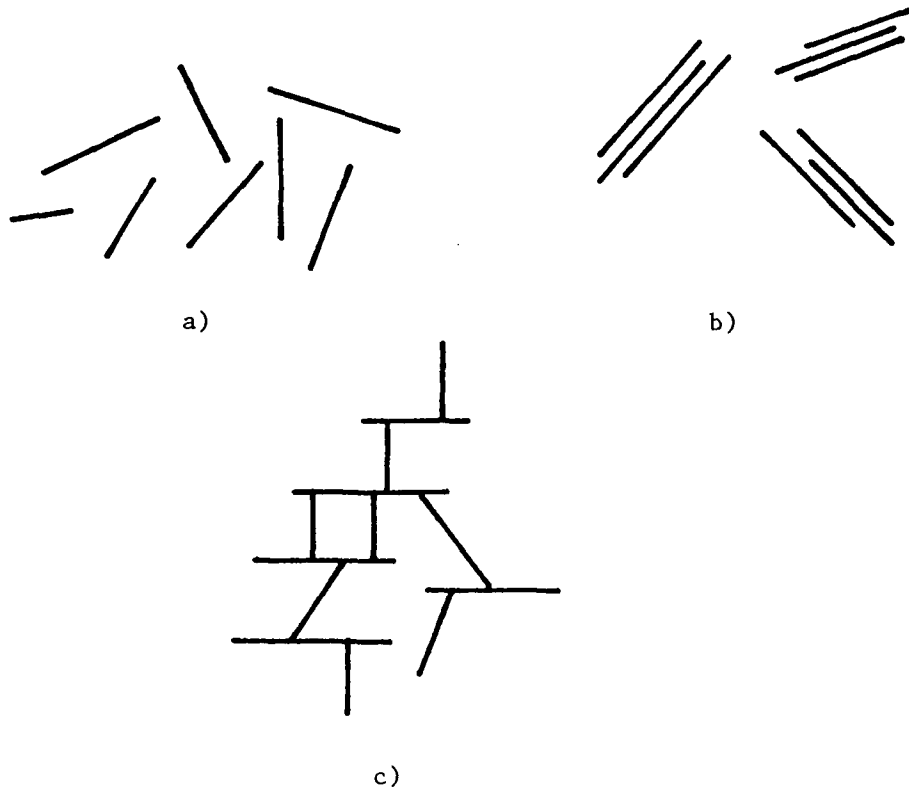


Fig. 2: Possible configurations of kaolin particles
a) deflocculated (dispersed)
b) deflocculated but associated
c) cardhouse structure

changing the pH. One should keep in mind the fact that montmorillonite platelets similarly have positive charge on the edges and negative charge on the faces. Because the thickness of the edges is so small (10\AA compared to $500\text{--}800\text{\AA}$ for kaolin), particles dispersed in 1:1 electrolytes at concentrations of 10^{-1}M to 10^{-4}M have electrokinetic properties which are entirely dominated by the charges on the faces as pointed out by Callaghan and Ottewill⁹ in an electrophoretic study of montmorillonite. Therefore, the edge charge of the kaolin platelets could be neutralized by adsorbed montmorillonite particles and the system will show less frame rigidity. This phenomenon is experimentally demonstrated in this work. It has been observed¹⁰ in some naturally occurring kaolin samples, known (by X-ray diffraction) to have a small percentage of montmorillonite and illite, that flocculation did not occur (judged visually) under the expected condition until the montmorillonite and illite were removed (by bringing to pH 10 to desorb these minerals, then separating by successive centrifugation).

B) Adsorption of organics on clay

It is estimated by Wangerdky¹¹ that sea water contains 0.5 to 1.2 mg/l of organic carbon, with the higher values found in the surface water. Amino acids, phenols, long chain organic surfactants, proteins and colloidal organic aggregates are the main constituents in this category.¹² In the adsorption of such organic solutes as phenols and related molecules, hydrogen bond formation is involved.¹² Similarly, in a study of adsorption of insecticides

on lake sediments, Lotse¹³ concluded that hydrogen bond or van der Waals interactions control the uptake.

Adsorbed molecules at high surface coverages may produce a steric barrier at the grain contact point, and this elastic layer will alter the resultant bulk modulus of the particles and also the density.

In the case of extreme pollution, long chain surfactants (e.g. alkyl ammonium ions), depending on the length of chain, will increase the basal plane separations of the clay minerals; and this phenomenon is called intercalation of organic materials in mica type layer silicates¹⁴. This will cause the destruction of the individual clay platelets which then form a gel.

C) Interparticle forces

Due to the crystalline structure of kaolin, the surfaces exposed exhibit charges, as mentioned above. When these particles are dispersed in electrolyte, a double layer is formed around them, depending on the strength of the electrolyte and the charge. There will be interaction when two particles approach near enough that their double layers overlap: attraction or repulsion depending on whether there are like or unlike charges on the near parts of the particles. Thus, the cardhouse structure is so prevalent; however, the face-to-face interaction will invariably be repulsion. When sound propagates in such dispersions, depending on the separation of such surfaces, an extra resistance to the displacement or

distortion of the particle frame will be experienced, and this may effect the velocity and absorption of sound.

III. THE THEORY OF THE INTERPARTICLE FORCES IN MARINE
COLLOIDS AND SEDIMENTS

To understand the conformational properties of sediments of small particles under various chemical conditions, we shall consider the potential energy of interaction of a pair of individual platelets or flocs of sediment particles. The total potential energy of interaction V of two interacting colloidal particles was considered to consist of two terms: when two particles approach each other, their electrical double layers overlap, leading to the repulsive energy V_R , while van der Waals-London attractive forces lead to attractive energy V_A . Thus,

$$V = V_R + V_A \quad (1)$$

The total potential energy of interaction as a function of distance of separation (H_o) between the surfaces of the particles is given in Fig. 3. At relatively large separations the combination of repulsion forces and London-van der Waals attraction yields a so-called secondary minimum. As the particles further approach each other, the potential energy curve shows a maximum. The larger the surface potential and the lower the ionic strength, the higher the maximum is. At close separations, Born repulsion and London-van der Waals attractions cause the deep primary minimum.

Although colloidal dispersions on thermodynamic grounds can

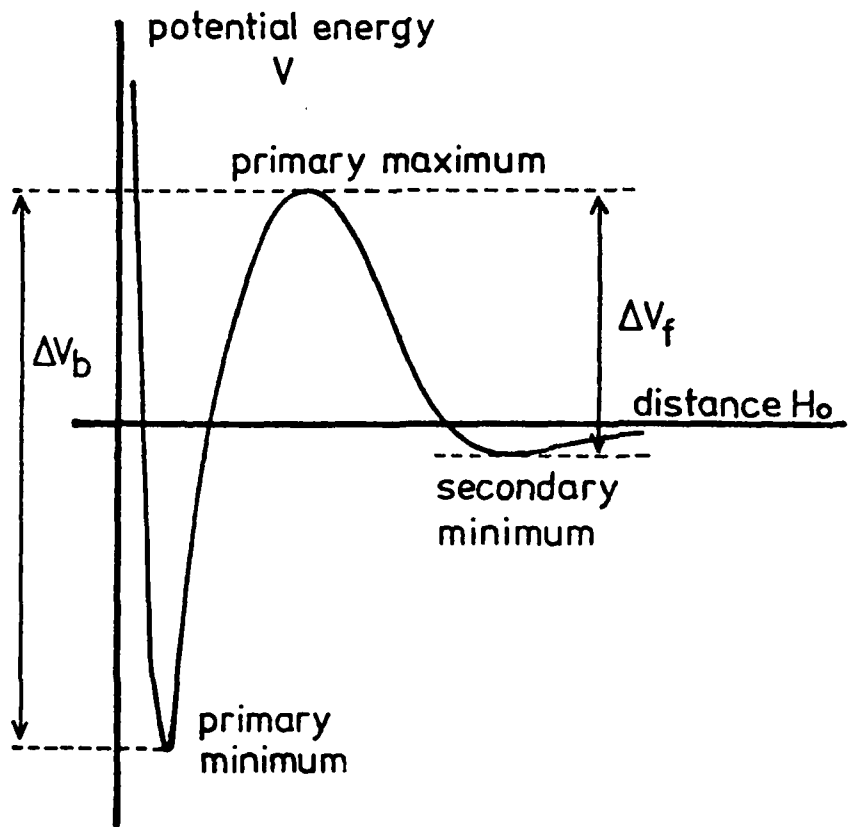


Fig. 3: Total potential energy of interaction between two particles as a function of separation

never be truly stable, most moderately concentrated dispersions tend to remain in the secondary minimum. To coagulate the system, ΔV_f energy barrier must be overcome. Similarly, to redisperse the particle, the ΔV_b barrier of peptisation must be overcome.

In the theory developed by Derjaguin, Landau, Verwey and Overbeck, commonly known as DLVO¹⁵ theory of the stability of colloidal particles, the assumption for the derivation of the electrical repulsion between two flat double layers is made so that during interaction the potential at the particle surface is kept constant. This then requires that when the particles come near to each other, their charge must decrease. However, it has come to be more widely accepted that the assumption of constant charge is more realistic. Therefore, the constant charge assumption during the interaction of the two particles at close separations is used. Fig. 4 is the potential diagram of two particles with interacting double layers.

The force per unit area for two interacting parallel planes at a separation H_0 can be calculated, assuming small surface potential, by using the linear Poisson-Boltzmann equation. It can be shown⁴⁹ that the potential mid-way between interacting plates y_m is given

by

$$y_m = y_0 \operatorname{csch}(\kappa H_0 / 2)$$

where

$$y_0 = \frac{ze\psi_0}{kT},$$

H_0 is the particle separation, z the valency of the ions, e the elementary charge, k Boltzmann's constant, T the absolute temperature,

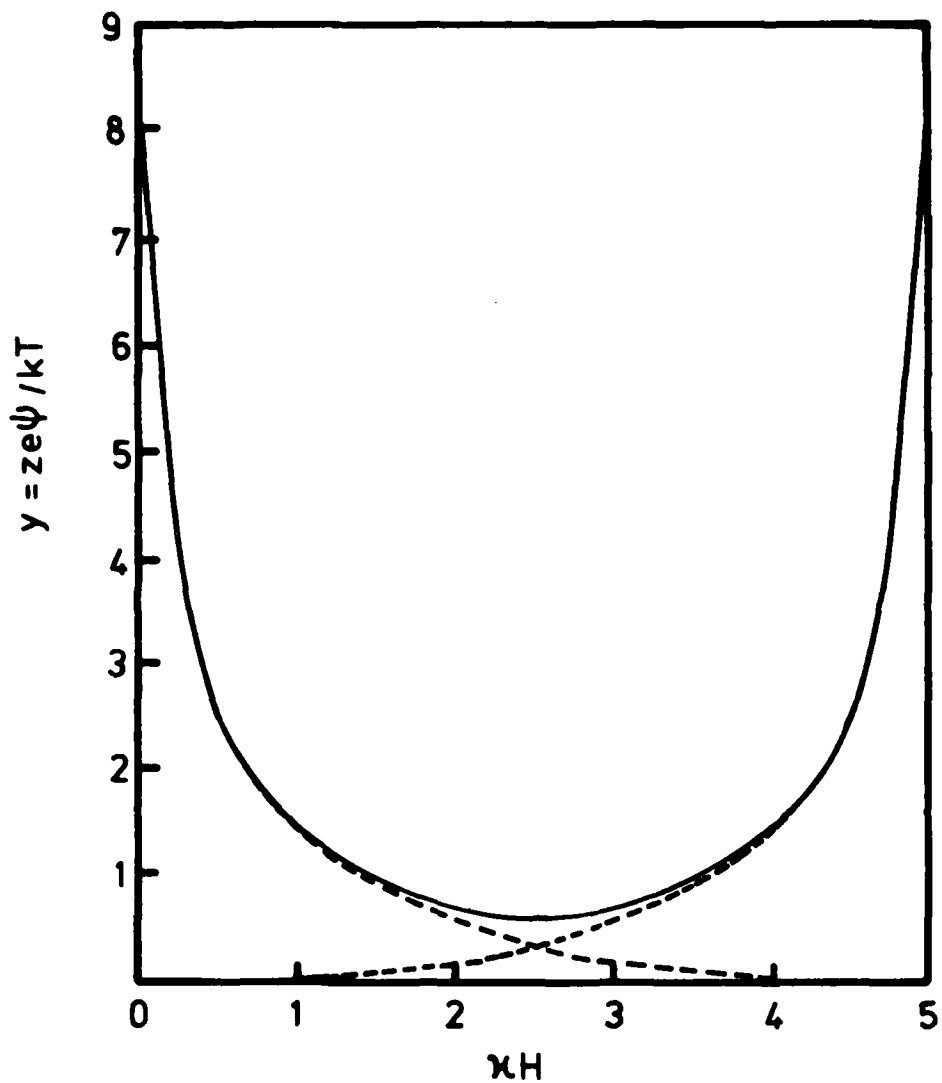


Fig. 4: Potential diagram of the interaction of two diffuse double layers as function of κH .

ψ_0 the potential at the surface, and κ is the Debye-Hückel reciprocal length,

$$\kappa^2 = \frac{2e^2nz^2}{\epsilon kT}$$

where n is the number of cations (or anions) per unit volume, and ϵ is the permittivity of the medium.

The force (per unit area) between the plates is given by¹⁵

$$F = 2nkT (\cosh y_m - 1) \quad (1)$$

This formula can be rewritten for values of y_m up to around 1,

$$F = nkTy_m^2 \quad (2)$$

therefore, for the constant charge case,

$$F = nkTy_0^2 \operatorname{csch}^2(\kappa H_0/2) \quad (3)$$

The energy of interaction between plane surfaces at a separation H_0 is given by

$$V_R = - \int_{\infty}^H F dH \quad (4)$$

Substituting for F from eq (3) and integrating gives

$$V_R = (2nkT/\kappa) y_0^2 [\coth(\kappa H/2) - 1] \quad (5)$$

Similarly, Hamaker¹⁶ has shown that the potential energy of interaction due to van der Waals-London attractive forces between two flat plates of thickness t is given by

$$V_A = - \frac{A}{12\pi} \left[\frac{1}{H_0^2} + \frac{1}{(H_0+2t)^2} - \frac{1}{(H_0+t)^2} \right] \quad (6)$$

where A is the Hamaker constant for interaction of the particles.

It has been shown¹⁷ that for several oxides in water, the values

of A lie between 3.5×10^{-13} and 8×10^{-13} erg. Using eq.(5) and (6), the total energy of interaction can be calculated for a pair of plates.

The linear approximation given by eq. (2) may be used to estimate the magnitude of the forces of face-to-face interaction of the kaolin plates at low surface potentials (around 25 mV). At high pH, kaolin particles show negative charge on both faces and edges.

The repulsion force involving edges of kaolin particles can be calculated by using the repulsive energy of interaction between two dissimilar spheres of radius a_1 and a_2 and potentials ψ_1 and ψ_2 given by Hogg et al.¹⁸ for constant potential

$$V_R^\psi = \frac{\epsilon a_1 a_2 (\psi_1^2 + \psi_2^2)}{4(a_1 + a_2)} \left[\frac{2\psi_1 \psi_2}{(\psi_1^2 + \psi_2^2)} \ln \left[\frac{(1 + \exp(-\kappa H_o))}{(1 - \exp(-\kappa H_o))} \right] + \ln (1 - \exp(-2\kappa H_o)) \right] \quad (7)$$

If one approximates the edges of clay particles to a sphere of radius a_1 and the faces to a_2 , the above formula can be used to calculate the forces between face to edge interaction of the clay particles.

For identical spherical particles, i.e. $a_1 = a_2 = a$; $\psi_1 = \psi_2 = \psi$, the equation (7) reduces to

$$V_R^\psi = \frac{\epsilon a \psi^2}{2} \ln \left[1 + \exp(-\kappa H_o) \right] \quad (8)$$

Later Weise and Healy¹⁹ show that the interaction at constant surface charge can be calculated using the method given by Frens²⁰.

The general equation for two dissimilar spheres is

$$v_R^\sigma = v_R^\psi - \frac{\epsilon a_1 a_2 (\psi_1^2 + \psi_2^2)}{2(a_1 + a_2)} \left[\ln(1 - \exp(-2\kappa H_o)) \right] \quad (9)$$

The above expression for two identical spheres after substituting eq. (8) for v_R is

$$v_R^\sigma = \frac{\epsilon a \psi_o^2}{2} \ln \left[\frac{1}{1 - \exp(-\kappa H_o)} \right] \quad (10)$$

Successful application of the above equation to the problem of the flow of polymer latices was reported by J.P. Friend and R.J. Hunter²¹ and qualitative agreement for latex microspheres was obtained by L.A. Spillmand and P.M. Cukor²² who applied the equations to the problem of deposition of particles under such forces. More recently Vincent, Young and Tadros²³ predicted the general trend of the coagulation of the negatively charged big polymer latices by positively charged small spherical particles, both covered with adsorbed polymer, using the above theory.

As pointed out by Hunter²¹, application of the above theory to the clay dispersions is extremely difficult because of the hetero-polar nature of the clay particles. Moreover, it is also almost impossible to estimate the interaction area of the clay particles because of their irregular shapes. However, the above theory will serve as a general guide in this attempt to estimate the effect of the interparticle forces on attenuation and velocity of the sound waves in sediments. Flegman, Goodwin and Ottewill²⁴ have

calculated some total potential energy of interaction for edge-edge, edge-face and face-face interactions, using the constant potential approach; this work did not include any comparison with experimental results. Barclay and Ottewill²⁵ and Callaghan and Ottewill⁹ made an attempt to compare calculated results for montmorillonite with compression experiments.

IV. THE THEORY OF THE ATTENUATION AND VELOCITY OF SOUND WAVES
IN CONCENTRATED COLLOIDAL DISPERSIONS AND SEDIMENTS

Although various theories have been proposed to explain attenuation and velocity of sound waves in concentrated dispersions, very few have been tested; and all of them are incomplete in the context of the colloid chemistry point of view. No existing theory takes into account the possible contribution of the electrokinetic properties of the interfaces to the attenuation and velocity of sound waves. Apart from McCann's empirical approach⁶, no interparticle force effects due to overlapping double layers were taken into account. The possible effect of double layer relaxation and counterion binding on absorption have not been considered.

Among the theories are Nesterov's²⁶ and Ament's²⁷ approach of complex density for the treatment of the velocity and absorption of sound in emulsions and dispersions. Nesterov considered the particles in a cubic array, composed of small cylinders whose axes coincide with the direction of propagation of sound. Contrary to Nesterov's model, Ament models the dispersion as a porous plug,

implying that particles are in contact with each other.

It has been shown by Allegra and Hawley²⁸ that the Epstein-Carhart theory²⁹ given for compressible emulsion droplets, taking into account scattering, viscous drag and heat conduction losses, can be extended to dispersions of solid particles. Allegra and Hawley obtained an explicit expression for the attenuation coefficient by assuming low ka values. They calculated, with the aid of a computer, the zero, first and second order coefficients of the reflected waves for particles. The computations are rather long, and the complete theory is applicable only to dilute dispersions. Recently Davies³⁰ extended the Epstein-Carhart theory for compressible particles in a liquid, considering the redistribution of the incident acoustic energy by multiple scattering.

For the present work, it is necessary to consider higher concentrations where formulae linear in concentration are not adequate. On the other hand, for clay, quartz and sand, heat conduction losses may be considered negligible. To further simplify the treatment for concentrated suspensions, we shall assume the particles to be incompressible, which appears to be a reasonable first approximation.

In this work we have extended the approximate theory of Rytov³¹ to concentrated dispersions of small, rigid spherical particles, and interparticle forces are introduced to the equation of motion.

To compare our explicit approach with that of McCann using the formula linear with concentration of Lamb, Rytov and Urlick³²,

this first order theory will be discussed first.

The first work on the attenuation of sound due to scattering and viscous drag losses was that of Lamb in 1932.³³ Lamb obtained an expression for the average work done, when a sphere oscillates in a viscous fluid, from the zero and first order terms in a spherical Bessel-function expansion for the velocity potential of the scattered waves. Lamb considered a dilute dispersion of particles with radius a small compared to the incident wavelength λ , and a system so dilute that no multiple scattering exists. He considered the loss mechanism associated with the scattering of the incident wave to infinity and also the loss mechanism due to the relative movement through the liquid.

The absorption equation for a single particle is

$$2\alpha = \frac{4}{9} k^4 a^4 \cdot \pi a^2 + \frac{4\pi}{k^2} H' \quad (11)$$

where $k = \frac{2\pi}{\lambda}$; λ is the wavelength of the sound and a is the radius of the particle;

$$H' = \text{real part of } \frac{iA_1(\delta - \rho)}{\delta - \rho + \frac{3\rho A_1}{k^3 a^3}} \quad (11a)$$

where ρ and δ are the densities of the fluid and particle respectively.

$$A_1 = \frac{-(3+3iha-h^2 a^2)k^3 a^3}{2h^2 a^2} = \frac{1}{2}(1+\frac{3}{2\sqrt{\xi}}) - i \frac{3}{4\sqrt{\xi}}(1+\frac{1}{\sqrt{\xi}}) \frac{k^3 a^3}{a^3} \quad (11b)$$

where

$$h = 1 - i \left(\frac{\omega}{2\mu} \right)^{\frac{1}{2}} \quad \text{or} \quad \sqrt{\xi} = \frac{\omega a^2}{2\mu}$$

and ω is the angular frequency.

Urick modified this expression writing s to represent the frictional forces proportional to the velocity of the particle relative to that of the fluid and σ for the inertial forces;

$$s \equiv \frac{9}{4\sqrt{\xi}} \left(1 + \frac{1}{\sqrt{\xi}} \right); \quad \tau \equiv \frac{1}{2} + \frac{9}{4\sqrt{\xi}} \quad (11c)$$

Writing σ for the ratio of densities δ/ρ , eq. (11), after substitution from eq. (11a) and (11b), becomes

$$2\alpha = \frac{4}{9} \underline{k}^4 \underline{a}^4 \cdot \pi a^2 + \frac{4}{3} \pi a^3 \underline{k}(\sigma-1)^2 \frac{s}{s^2 + (\sigma + \tau)^2} \quad (12)$$

The first of the two terms on the right is the scattering loss produced by small rigid spherical particles free to move in the sound field, and the second term is a frictional loss due to the relative motion through suspending fluid exhibiting viscosity. Urick also approached the problem of calculating the viscous losses in suspensions from another theoretical point of view and obtained the same viscous term as in eq. (12). He wrote the equation of motion of a single particle in a sound field using the force exerted on a spherical pendulum swinging in a viscous fluid with an instantaneous velocity U . This force was originally given by Stokes:³⁵

$$\begin{aligned} F &= -\left(\frac{1}{2} + \frac{9}{4\sqrt{\xi}} \right) m_L \dot{U} - \frac{9}{4\sqrt{\xi}} \left(1 + \frac{1}{\sqrt{\xi}} \right) m_L \omega U = \\ &= -\tau m_L \dot{U} - s m_L \omega U \end{aligned} \quad (13)$$

where m_L is the apparent mass (the mass of fluid displaced by the sphere). This force is complex. The first term on the right hand side of the equation represents an addition to the inertia of the sphere and the second term is a drag force proportional to velocity.

For the present purpose, U represents the velocity difference between particle and fluid; $U = v - u$. The equation of motion is then:

$$F = m_p \dot{v} - m_L \dot{u} = -\tau m_L \dot{U} - s m_L \omega U$$

On replacing \dot{v} by $\dot{U} + \dot{u}$ and writing $\sigma = \frac{m_p}{m_L}$, this becomes, for a sinusoidal motion,

$$(\sigma + \tau) \dot{U} + s U \omega = -i \omega (\sigma - 1) u_o e^{i \omega t} \quad (14)$$

The solution of this equation is

$$U = \frac{(1 - \sigma)}{[s^2 + (\sigma + \tau)^2]^{\frac{1}{2}}} u_o e^{i(\omega t + \theta)}; \quad U = U_o \exp i(\omega t + \theta);$$

$$\frac{U_o}{u_o} = \frac{(1 - \sigma)}{[s^2 + (\sigma + \tau)^2]^{\frac{1}{2}}} \quad \text{and} \quad \tan \theta = -\frac{s}{\sigma + \tau} \quad (15)$$

where U_o is relative velocity amplitude of the particles and u_o = velocity amplitude of the solid. Since

$$I = I_o \exp -\theta \underline{k} s \left(\frac{U_o}{u_o}\right)^2 \quad (15a)$$

where ϕ is volume fraction, the intensity absorption coefficient becomes

$$2\alpha = \phi \underline{k} (\sigma - 1)^2 \frac{s}{s^2 + (\sigma + \tau)^2} \quad (16)$$

We shall call this equation L.R.U. approximate equation.

Rytov³¹ approached the problem by writing a set of equations for u and v , taking into account the fact that as particles are crowded

together, the volume fraction is altered.

Using the subscripts 0 to denote the equilibrium condition, and 1, the small deviations from equilibrium,

$$\rho = \rho_0 + \rho_1, \text{ and } \phi = \phi_0 + \phi_1$$

The particles are considered incompressible; therefore, $\delta = \delta_0$.

Conservation of mass dictates that the rate of increase of mass per volume in the x direction is the negative gradient of velocity in that direction. This is expressed separately for the liquid:

$$\frac{\partial}{\partial x}[(1-\phi_0)\rho_0 u] = -\frac{\partial}{\partial t}[(1-\phi_0)\rho_1 - \rho_0\phi_1] \quad (17)$$

and for the particles for which the density δ is considered constant:

$$\frac{\partial}{\partial x}\phi_0 \delta v = -\frac{\partial}{\partial t}\delta\phi_1 \quad (18)$$

Acceleration is proportional to the gradient of pressure which, in turn, is proportional to the gradient of density;

$$\frac{\partial}{\partial t}[(1-\phi_0)u + \phi_0 \delta v] = -\frac{\partial p}{\partial x} = -c^2 \frac{\partial \rho}{\partial x} \quad (19)$$

The relative motion of the particle was determined by an equation which, when transformed, is identical to that used by Urick. The ratio B of the velocities of particle v and medium u (i.e., the König³⁶ equation) is

$$\frac{v}{u} = B = \frac{1 + \sqrt{\xi} + i\sqrt{\xi}(1+2/3\sqrt{\xi})}{1 + \sqrt{\xi} + i\sqrt{\xi}(1+b\sqrt{\xi})} \quad (20)$$

where $b = \frac{2}{9}(1+2\sigma)$.

This may be expressed in terms of s, τ , and σ ; thus $B = 1 - \frac{\sigma-1}{\sigma+\tau-i s}$. (20a)

From the set of equations (17-20) and the relation $u = Bv$, we can write as follows:

$$\frac{\partial^2 u}{\partial x^2} + \frac{\omega^2}{c^2}(1-\phi_o) \cdot \frac{1-\phi_o + \sigma\phi_o B}{1-\phi+\phi B} u = 0 \quad (21)$$

The solution to eq. (21) is given in the form $u = e^{-(\alpha + i \frac{\omega}{c})x}$; α represents the absorption and c represents the phase velocity.

Rytov in 1938 never used the complete equation (21) but rather introduced several approximations which resulted in an equation identical (when transformed) with that derived by Urick in 1948.

Barrett-Gultepe et al.⁷ compared the approximate equation (L.R.U.) with that of Rytov and with Urick's experimental results; however, the formula still contained one approximation.

Numerical values of absorption and phase velocity have been calculated from eq. (11) with the aid of a computer. Fig. 5 shows the comparison of the L.R.U. approximation for dilute dispersions with the Rytov complete formula. Note that the form of the absorption curve now shows a maximum, as do the experimental results.

IV.A Velocity

Although it is possible to obtain the velocity from the complex wave number along with absorption, there are various treatments for velocity alone. The earliest treatment was given by Wood,³⁷ where the values of density and compressibility are simply considered as the average of the two components:

$$\beta_{PL} = n\beta_L + (1-n)\beta_P \quad (22)$$

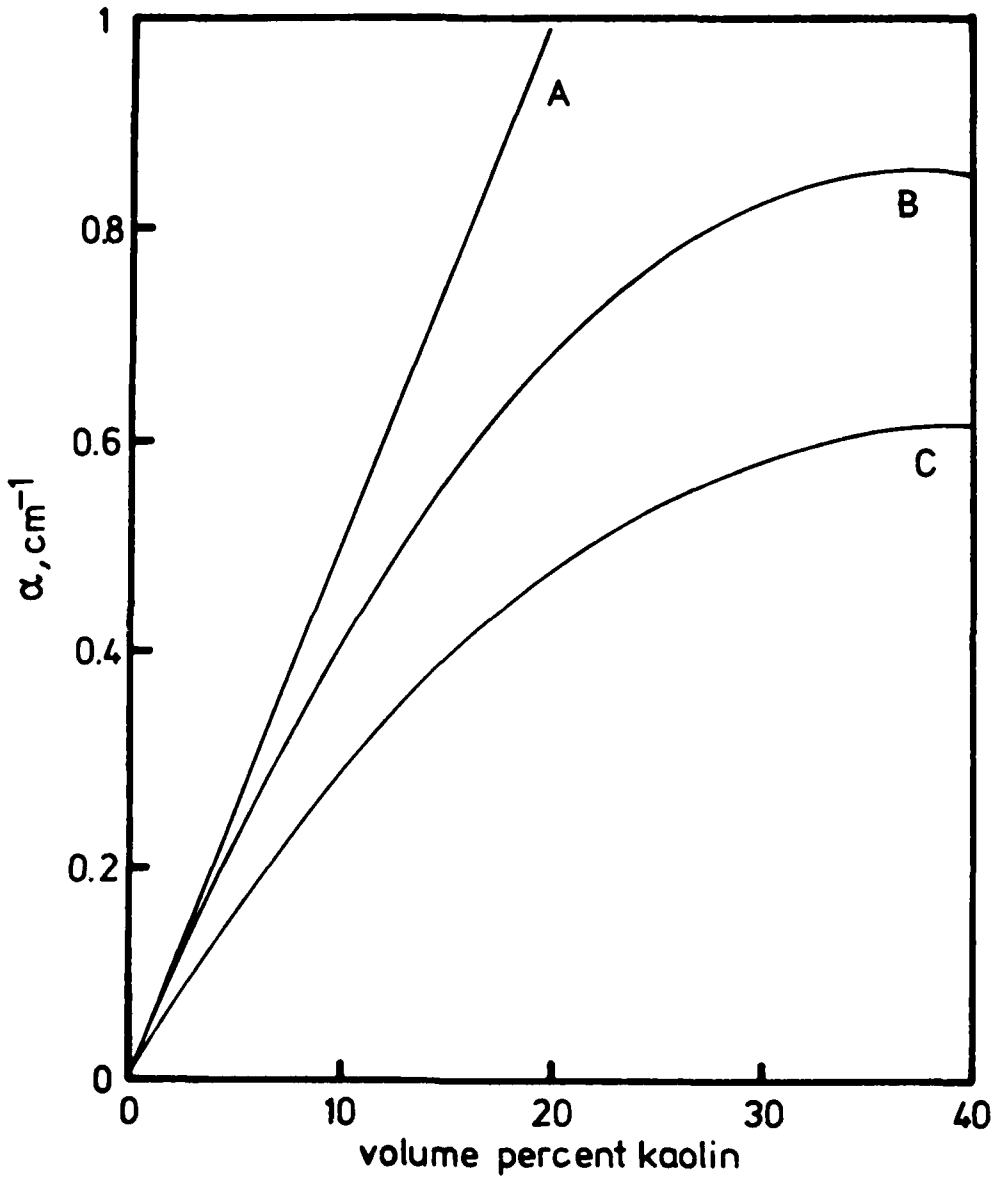


Fig. 5: Calculated absorption values for kaolin dispersions in water at 1 MHz at 25°C.
A. LRU eq. (16) assuming particles of 1μ diameter
B. Rytov eq. (21) assuming particles at 1μ diameter
C. Rytov eq. (21) assuming the particle size distribution given in Fig. 7

or expressed as the bulk modulus

$$K_{PL} = K_L K_P / [n(K_P - K_L) + K_P] \quad (23)$$

and for the density

$$\rho_{PL} = n\rho + (1-n)\delta \quad (24)$$

where n is the volume of pore space occupied by water. From the relation $c = \left(\frac{1}{\beta\rho}\right)^{1/2}$ we obtain Wood's equation:

$$c = \left(\frac{1}{[n\beta_L + (1-n)\beta_P][n\rho + (1-n)\delta]} \right)^{1/2} \quad (25)$$

The assumption implicit in this is that the particles and medium move together. As a result, it is a reasonable formula for low frequencies, or for systems with particles of density similar to the medium (such as polymer colloids). Hamilton,³⁸ considering combined bulk moduli of sediment water mixtures, found this formula did not explain the compressional velocity observed in sediments. He pointed out that either K was not adequately defined or frame rigidity is present. He concluded that deviations from Wood's formula are due to the frame bulk modulus (or skeletal bulk modulus). For frame bulk modulus, he proposed to use the Gassman⁵ closed system bulk modulus in which water within the skeleton does not "circulate" under the influence of propagation of elastic waves. The closed system bulk modulus is given by

$$K = K_P \frac{K_f + Q}{K_P + Q}; \quad Q = \frac{K_L (K_P - K_f)}{n(K_P - K_L)} \quad (26)$$

where K_f is the frame bulk modulus of Gassmann.

In order to calculate the "closed system bulk modulus", it is necessary to know porosity, bulk modulus of the water, bulk modulus of the mineral grain and the frame bulk modulus. Compressional wave velocity measurements are not sufficient to evaluate these unknowns (see Hamilton³⁸). The nature of the forces causing this frame bulk modulus is not discussed.

Later Urick and Ament³⁹ took into account the influence on velocity of the fact that particle and medium do not move together unless their densities are the same, and showed that the result of this relative motion for heavy particles is to increase velocity. They did not give as an example the effect on clay suspensions. Ament²⁷ later treated the sample as a porous plug, i.e. as a fixed framework, and introduced the complex density. Nesterov²⁶ used a similar complex density concept for velocity and attenuation as mentioned earlier.

Hampton⁴⁰ applied Ament's theory to velocity data of kaolin in the 50-200 kHz range. Ament's theory underestimated the velocity ratios in the low concentration range and overestimated them at high concentrations. The predicted velocity dispersion is of the order of 1% for a 20 volume percent kaolin suspension between 50 and 200 kHz; the experimental dispersion is of this order but unfortunately the data of Hampton used for comparison shows considerable scatter.

IV.B McCann's treatment

McCann⁶ introduced a force into the first order theory (Lamb-Rytov-Urick) based on a treatment given by Kittel.⁴¹ Kittel considered lattice vibrations assuming a row of charged particles, as shown in Fig. 6.

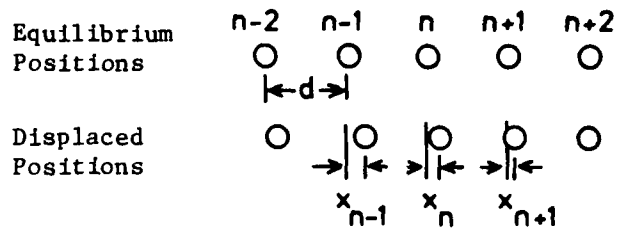


Fig. 6: The vibrations of a line of charged particles

When a wave travels along the line of charged particles, resulting in a displacement of one particle relative to its neighbors, the n^{th} particle will experience a force F_n :

$$F_n = f(x_{n+1} - x_n) - f(x_n - x_{n-1}) \quad (27)$$

where f is the force constant.

Kittel showed that this force can be related to the displacement of the particle and particle spacing and the wavelength:

$$F_n = x_n 4 \sin^2 \left(\frac{kd}{2} \right) \quad (28)$$

where x_n is the displacement of the particle. When $k \ll d$,

$$\sin^2 \left(\frac{kd}{2} \right) \rightarrow \frac{k^2 d^2}{4} \quad (29)$$

and finally

$$F_n = k^2 d^2 f x_n$$

McCann introduced this force in the equation of motion of

particles given by Urick (see eq. (6)) by writing the equation in terms of displacement:

$$m_p \ddot{x}_n + k^2 d^2 \beta_n = -\tau m_L \ddot{x}_u - s m_L \omega \dot{x}_u + m_L \ddot{x}_L \quad (30)$$

where x_n is the particle displacement from its equilibrium position, x_u is the particle displacement relative to the fluid, and x_L is the fluid displacement. This leads to the relative velocity of particle to liquid in Urick's form as follows:

$$\frac{U_o}{u_o} = \frac{\sigma - 1 - fd^2/m_L c^2}{[(\sigma + \tau - fd^2/m_L c^2 + s^2)^{1/2}]} \quad (31)$$

In Urick's linear approximation this is related to the absorption coefficient as shown earlier (see eq. (16)). Hence,

$$2\alpha = \frac{\phi \omega s}{c} \frac{[\sigma - 1 - fd^2/m_L c^2]^2}{[\sigma + \tau - fd^2/m_L c^2 + s^2]^2} \quad (32)$$

He considered that the force constant should be given by the derivative of the Coulombic force:

$$f = \frac{Rq^2 a^4}{d^3} \quad (33)$$

where R is a constant and q is the charge per unit area on each particle. The values of d were then related to concentration using

$$d = \frac{a (\frac{4}{3}\pi)^{1/3}}{\phi^{1/3}} \quad (34)$$

Then

$$fd^2/m_L c^2 = \frac{Rq^2 a^2}{d^3} \cdot \frac{d^2}{m_L c} = Rq^2 a^2 \phi^{1/3} = P\phi^{1/3} \quad (35)$$

where P is a constant,

and thus,

$$2\alpha = \frac{\phi\omega s}{c} \frac{(\sigma - 1 - P\phi^{1/3})^2}{(\sigma + \tau - P\phi^{1/3}) + s^2} \quad (36)$$

He then found the value of his constant P best fitting Urick's data to be 1.7.

IV. C Present treatment

The McCann treatment of interparticle forces ignores the screening effect of the ionic double layer of the particles in electrolytes. A more appropriate approach is provided by DLVO theory described in section II. This theory no longer leads to the simple relationship with distance assumed by McCann.

The second consideration that interferes with the use of the simplified expression with $\phi^{1/3}$ for clay is the geometrical form of the clay particles. Platelets, if randomly oriented, will come into contact with each other with increasing particle concentration much earlier than predicted on the basis of spherical particles. It is likely that the clay particles adopt different configurations at different concentrations, high concentrations favoring parallel configurations (assuming deflocculated dispersions).

The third modification to the theory is application of the force constant approach to the Rytov formula instead of the linear approximation with concentration. In the case of complete deflocculation, it could be assumed that most particles orient themselves parallel to each other because of the dominating face-to-face electrostatic repulsion, particularly for higher concentrations. Under

these circumstances the face-face and edge-edge repulsion must be considered. However, complete deflocculation cannot be achieved and some interaction, therefore, exists.

The force can be related to the potential energy of interaction:

$$F = -\left(\frac{\partial V}{\partial H_o}\right)_{\psi_{H_o/2}, \psi_o} \quad (37)$$

and the force constant:

$$f = \frac{\partial^2 V}{\partial H_o^2} \quad (38)$$

Therefore, for face-to-face interaction the force constant can be found from eq. (5) in section II for parallel plates:

$$f = \frac{d^2 V}{dH_o^2} = 2nkTy_o \operatorname{csch}\left(\frac{\kappa H_o}{2}\right) \coth\left(\frac{\kappa H_o}{2}\right) \cdot \frac{\kappa}{2} \quad (39)$$

and approximating the edge-to-edge interaction to that of two spheres, from eq. (10) in section II we can write for the force:

$$F = \frac{dV}{dH_o} = -\frac{\epsilon a \psi^2}{2} \cdot \frac{\kappa e^{-\kappa H_o}}{1 + e^{-\kappa H_o}} \quad (40)$$

and for the force constant f:

$$f = \frac{d^2 V}{dH_o^2} = \frac{\epsilon a \psi^2}{2} \cdot \frac{\kappa^2 e^{-\kappa H_o}}{(1 + e^{-\kappa H_o})^2} \quad (41)$$

The contribution Y to eq. (21) will be given by

$$Y = fd^2/m_L c^2 \quad (42)$$

Y is equivalent to the term $\rho\phi^{1/3}$ used by McCann, but now no assumption is made as to the relationship of d and f to concentration.

The term Y is inserted into equation (21) in a manner similar to McCann's treatment:

$$B = 1 - \frac{\sigma - 1 - Y}{\sigma + \tau - Y - i s} \quad (43)$$

The value of B is then used to find α and c from equation (21).

The choice of particle spacing representing a realistic model is difficult. A model frequently used to assume the solid material lies in solid layers of thickness equal to that of a single particle. This will necessarily lead to an overestimate of the quantities H_0 and d for any given volume concentration.

V. EXPERIMENTAL

V.A Montmorillonite

The montmorillonite was a sample of yellow Brock from Wyoming kindly donated by Dr. W. Moll of Georgia Kaolin Company, N.J. For the preparation, 30g of this material was mixed with 1 liter of laboratory distilled water in a Waring blender for 5 minutes. Then 1 cm³ of 30% hydrogen peroxide per 100g of montmorillonite was added, and the mixture was heated to 80°C, held at this temperature for 0.5 hours and cooled. After 24 hours storage the dispersion was decanted and the top fraction of sediment (~5%) saved. The dispersion was stored a further 3 weeks and decanted in order to separate more of the impurities. At the end of this period the dispersion was centrifuged at 16300g for 1 hour. The solids then separated into two distinct layers. The top layer was the montmorillonite and was removed as a golden-yellow gel; the bottom layer,

containing impurities, was discarded. The supernatant also contains a certain amount of montmorillonite.

Electron micrographs obtained by Case showed that the particles in the gel layer were 450-600 Å in diameter, while the particles in the supernatant were 150-185 Å.* The mass fraction of the gel was determined as 3.7% wt.%. The gel, after preparation, was prevented from drying because when once dried, it is very difficult to rehydrate.

V.B Kaolin

A sample of batch III "no-chemical refined" kaolin KLO/1783 was kindly provided by Dr. Jepson of English Clays Lovering Pochin Co. Ltd., Cornwall, England. Information on some physical and chemical properties pertaining to this sample was also supplied by Dr. Jepson and is given in Table I, and the particle size distribution (Stocks diameter) is given in Fig. 7.

The sample was either used in the condition as received, or for certain experiments (to be reported in future reports), was given the following preparation to obtain electrolyte free clay. In this procedure 200g kaolin was dispersed in distilled water and enough NaOH was added to deflocculate it. Then 1 cc of 30% H₂O₂ per 100g clay was added and the mixture was stirred continuously for 1 week. The sample was then centrifuged and the clay was

* This work was done by Y. Chonde, a graduate student working on this contract.

TABLE I

Batch III, No-Chemical Refined Clay

Particle Size

Above 10 μ	0.1%
Above 5 μ	5%
Below 2 μ	80%

Reflectance Against Magnesium Oxide

93% at 458nm
95.3% at 573nm

Specific Surface Area (nitrogen) 9.8m²/g

Cation Exchange Capacity (ammonium acetate saturation) 4.0 meq/100g

X-Ray analysis

Kaolinite	97 wt.%
Mica	3 wt.%
Other minerals	none
Crystallinity index	1.24

Chemical analysis

SiO ₂	46 wt.%
Al ₂ O ₃	39 wt.%
Fe ₂ O ₃	0.39 wt.%
TiO ₂	0.21 wt.%
CaO	0.07 wt.%
MgO	0.08 wt.%
K ₂ O	0.50 wt.%
Na ₂ O	0.1 wt.%
Loss on ignition	13.6 wt.%
Organic Carbon	0.04 wt.%

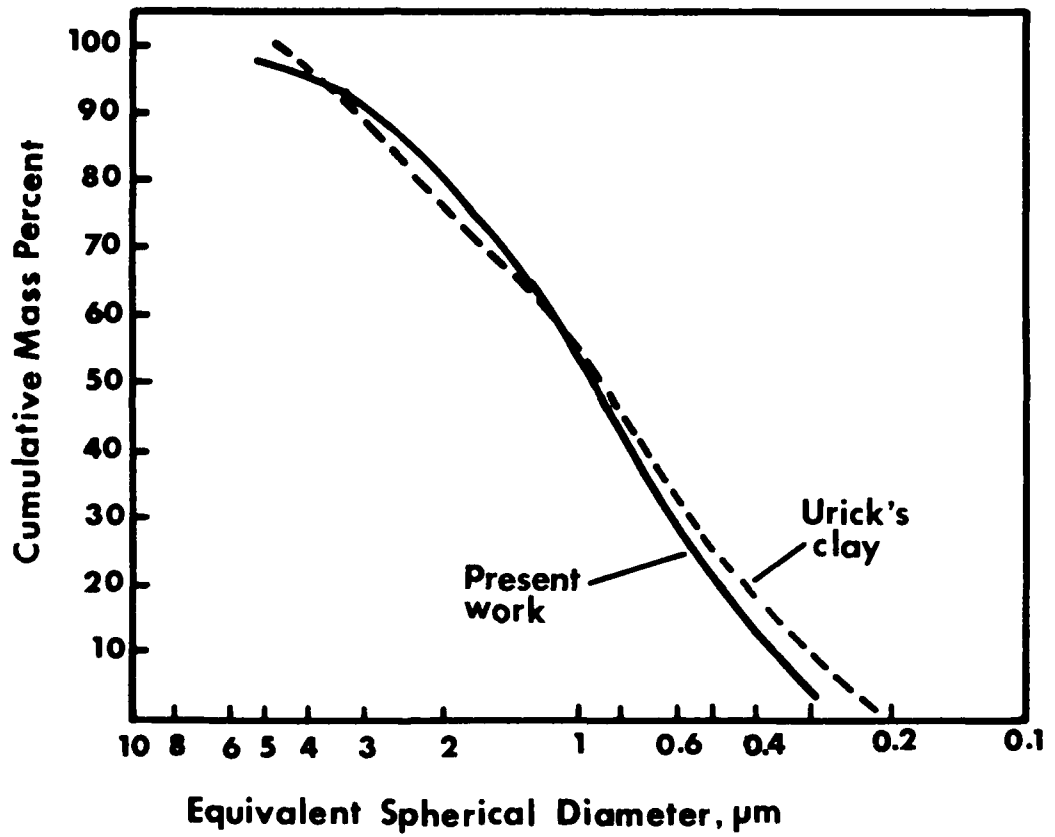


Fig. 7: Particle size distribution of the kaolin sample used in the present work. That of the kaolin used by Urick³⁴ is included for comparison.

redispersed in 1M NaCl + 10^{-3} M HCl. This procedure was repeated until the Al^{+3} concentration in the supernatant was around 10^{-5} M. The resulting Na kaolinite was then washed with distilled water 6 times (by centrifuging and then redispersing). Electrolyte free clay was separated by filtration and dried at 70°C.

In this work deflocculation was accomplished either by the traditional method of changing pH, using Na-pyrophosphate or sodium hydroxide or by coating the particles with a polymer introducing steric stability. For this purpose 72% hydrolyzed PVA (Alcotex) was used, kindly donated by Dr. D. Rance, ICI England. The poly(vinyl alcohol/acetate) block copolymer (PVA) is known to strongly adsorb on surfaces. For the sample used here, adsorption was known to be non-Langmuirian. Because of the hydrophobic and hydrophilic nature of the polymer, this type of material has been extensively used to stabilize two-phase systems, such as emulsions and dispersions, with hydrophilic end toward the solvent. In this work concentrations of PVA were added which are known to give a thickness of 30nm.⁵⁰

V.C Velocity and attenuation measurements

Velocity measurements were done at a single frequency of 2 MHz with an ultrasonic interferometer (Schall-Interferometer, type SI-2000). The driving signal was obtained from a crystal controlled oscillator. Standing waves were established between the driving transducer and traveling reflector. The wavelength of the sound waves was determined by observing the distance of travel of the reflector between successive minima of the driving current of the

transducer. The interferometer was thermostated so that during measurements the temperature was kept constant within $\pm 0.02^\circ\text{C}$. All measurements were done at 25°C . The velocity value obtained for pure water, after correction for small temperature variations, was $1.4975 \pm 0.0005 \times 10^5 \text{ cm s}^{-1}$, compared with the $1.4970 \times 10^5 \text{ cm s}^{-1}$ value found by Greenspan and Tscheigg.⁴²

Absorption measurements were made with a pulse send-receive apparatus.⁴³ Measurements were made at 1 and 5 MHz. With the samples used in this work, the absorption was so high that any diffraction errors in the measured attenuation are insignificant.

Attenuation measurements were done as follows: the height of the demodulated electric signal for the received acoustic pulse was matched to a comparison pulse obtained from a signal given with a precise attenuator.

It is known that air bubbles trapped in suspensions and liquids cause serious error in velocity and absorption measurements. To prevent this the following procedure was used. The dispersion was cavitated by an ultrasonic cleaning unit at 20 kHz capable of delivering 400W, while under reduced pressure ($\sim 30\text{-}50\text{mm}$). It was found that the results did not differ from those when the sample was subjected to sound waves at 10 kHz with a Raytheon magnetostrictive generator which is a more powerful treatment than the previous one. It has been pointed out that subjecting the clay dispersions to ultrasonic waves can alter the particle size distribution.⁴⁴ In this study samples were ultrasonicated and degassed

until they showed sufficient fluidity and no further air bubbles came out. No dependence of the measurements on the sonication time was found, and thus it is unlikely that any significant change was produced in the particle size.

Using kaolin as received, velocity measurements were done in kaolin dispersions as a function of concentration. The clay samples were deflocculated with a sufficient amount of sodium pyrophosphate solution. Deflocculation was achieved at approximately pH 9.2, regardless of concentration. The results are plotted as a ratio of the velocity with that of the supernatant. The supernatant was obtained by centrifugation. However, it was found that the same velocity was obtained with an artificial supernatant, i.e. water containing the same concentration of pyrophosphate as was added to the clay suspension.

In order to check the efficiency of pyrophosphate as a deflocculant, the following experiment was done. After the dispersions were deflocculated with pyrophosphate, the required quantity of PVA was added to the dispersions, and the velocity measurements was repeated. No difference was found.

Absorption measurements were made with kaolin samples deflocculated with sodium pyrophosphate over approximately the same range of concentrations at 1 MHz and 5 MHz.

Velocity measurements were made in mixtures of montmorillonite and kaolin in the absence of deflocculant. All suspensions were approximately total 10% by volume. The pH of the mixed dispersions

varied from 5.9 for the pure kaolin to 7.5 for the dispersion with maximum montmorillonite. After determination of the volume fraction by weighing, drying and reweighing, the velocity values were corrected to 10% by volume of solids, to aid comparison, and are plotted in this way in Fig. 8. The density values were taken as 2.65 for the montmorillonite and for kaolin on the basis of the typical values listed in the literature.⁴⁵

The range of concentrations of montmorillonite was chosen from considerations of the amount that would be required to cover the edge areas of the kaolin particles, although this could not be estimated with any accuracy.

VI. DISCUSSION AND RESULTS

The absorption results are shown for 1 MHz and 5 MHz (Figs. 9,10). For 1 MHz the results of Urick³⁴ are included since the clay samples for both sets of data have a similar size distribution (although obtained from different sources) and were both deflocculated with sodium-pyrophosphate. It is seen that results are in fair agreement. Unfortunately, other results of Urick cannot be so easily compared because of the difference of frequency. The theoretical curves using the Rytov equation are given in the figures, assuming a uniform particle size of 1μ , and various density ratios (particle/liquid). The velocity results are shown in Fig. 11 with the curve for Wood's formula (eq. (22)), assuming incompressible particles for comparison.

The choice of the parameters (particularly particle density and size) to use in the calculations is not straightforward and a discussion

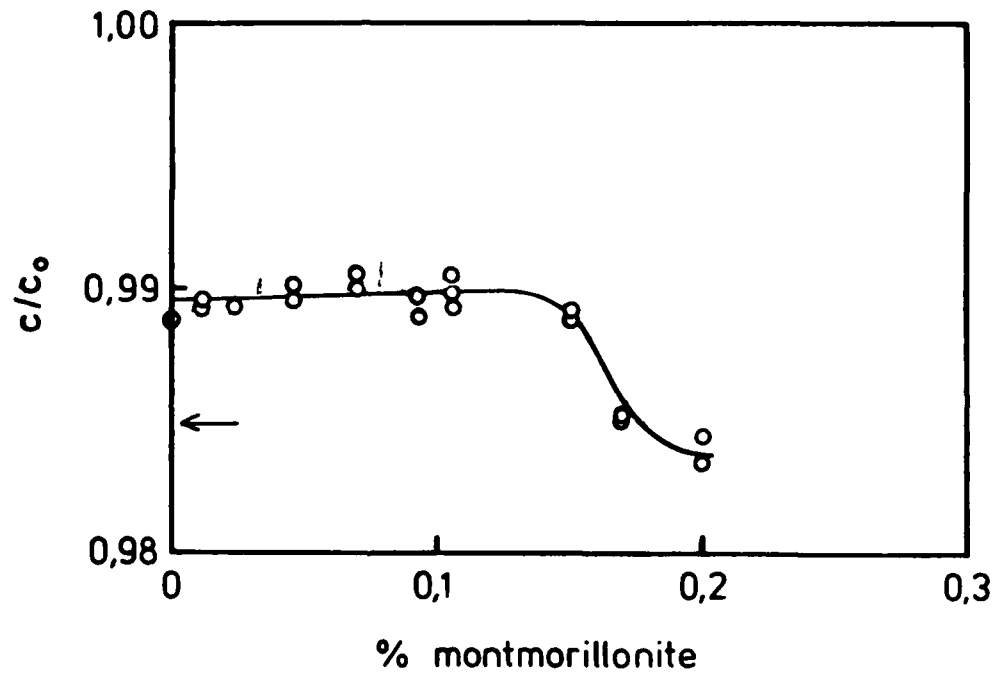


Fig. 8: Velocity ratio measured for a 10% by volume kaolin suspension with increasing amounts of montmorillonite. The arrow indicates the velocity ratio of 10% by volume kaolin deflocculated with sodium pyrophosphate at pH = 9.2.

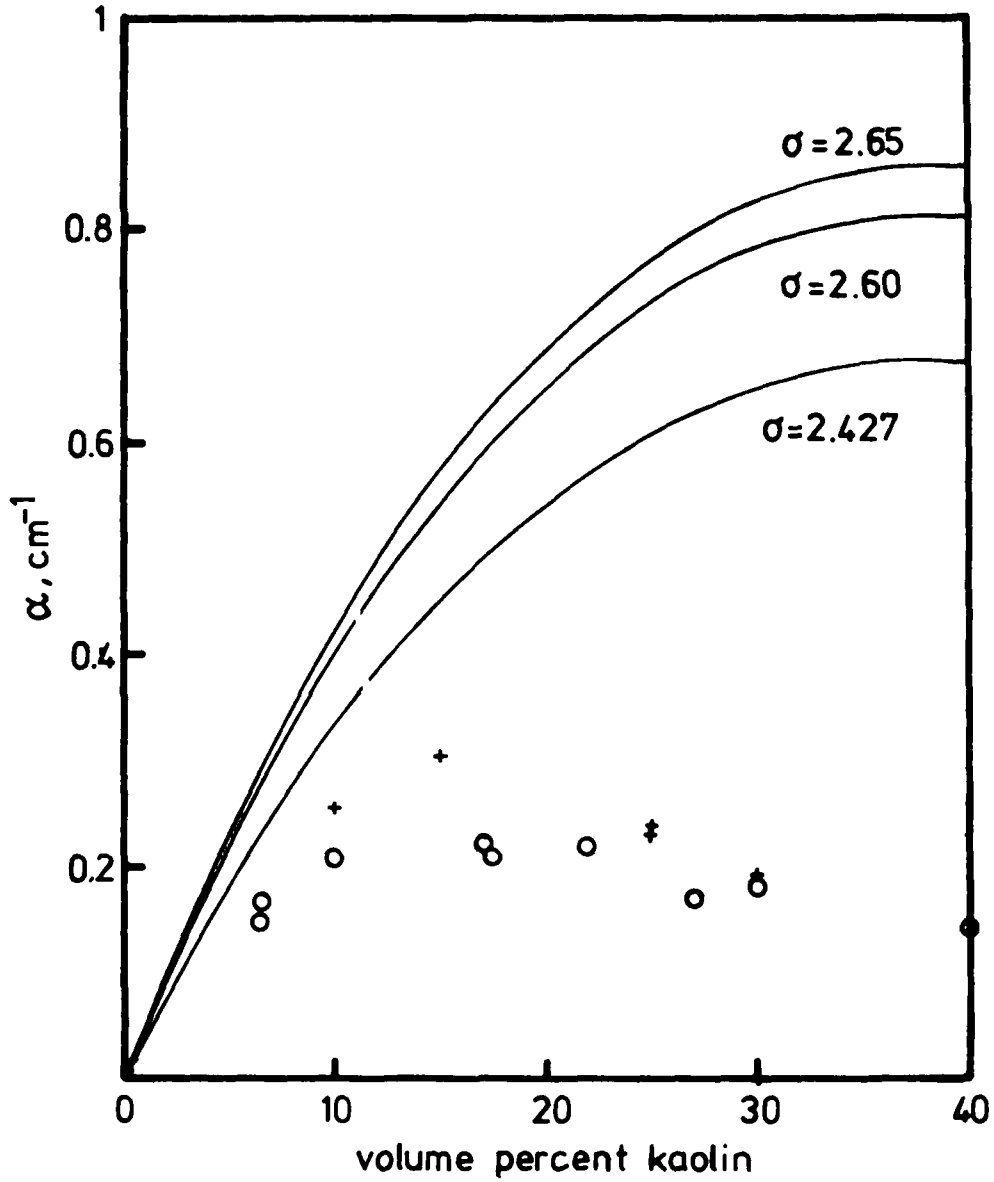


Fig. 9: Acoustic absorption values for kaolin suspensions at 1 MHz. Solid lines are values calculated using Rytov's eq. (21) for the particle to liquid density ratios given on the curves. Experimental values: + = present work; o = Urick¹⁶

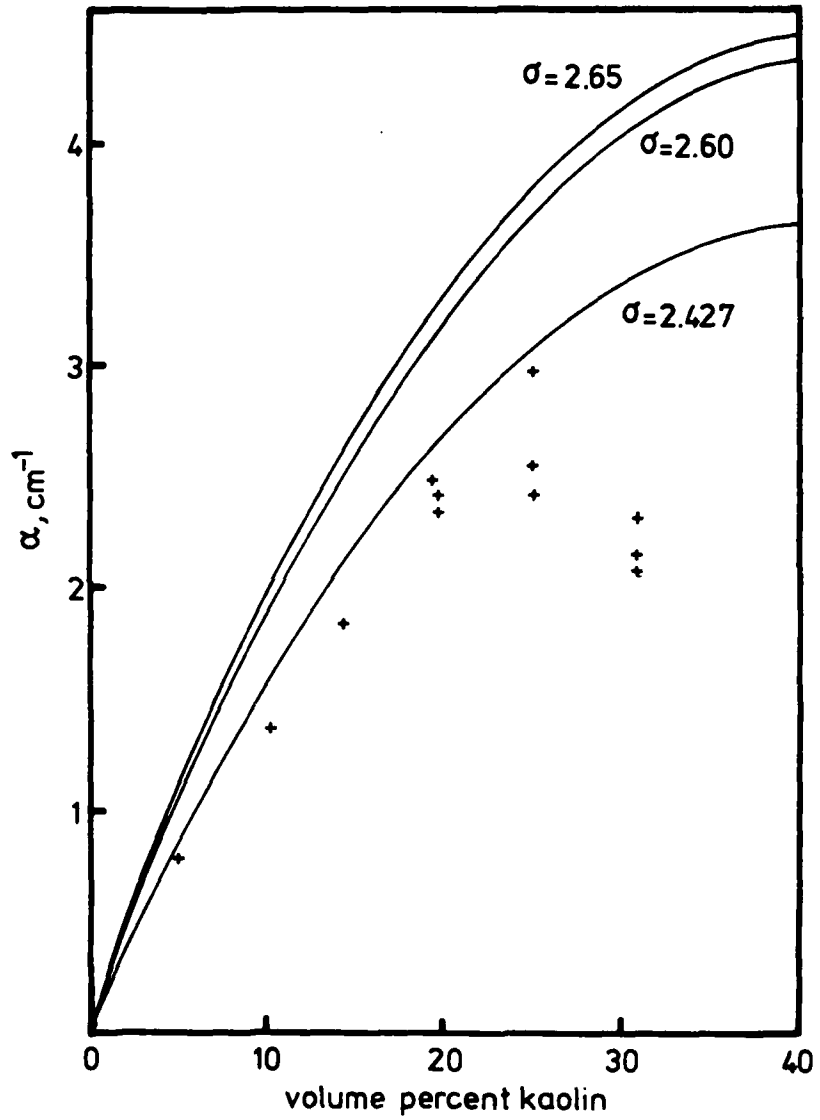


Fig. 10: Acoustic absorption values for kaolin suspensions at 5 MHz. Solid lines are values calculated using Rytov's eq. (21) for the particle to liquid density ratios given on the curves. Experimental values: + = present work

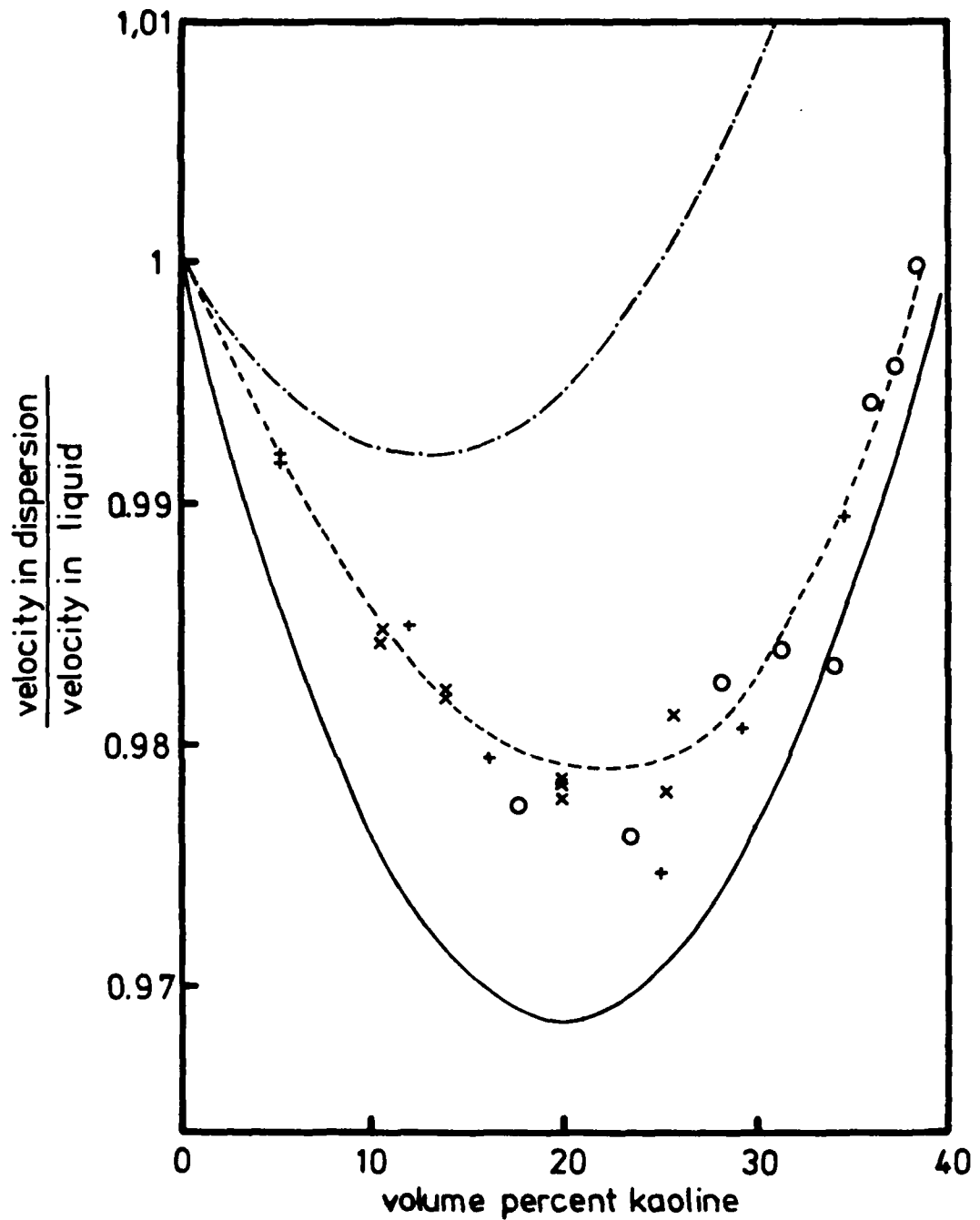


Fig. 11: Velocity of sound in kaolin dispersions at 2 MHz.
— : calculated by Wood's formula, eq. (22)
-·- : calculated by Rytov's formula, eq. (21)
--- : as above with the correction for interparticle forces, Y , given in Fig. 12
Experimental points: o, x kaolin deflocculated at pH 9.2 with sodium pyrophosphate: o = concentrated form of the dispersions represented by x; + = kaolin as above, then coated with PVA

follows.

The density of kaolin taken for acoustic calculations in the literature have been 2.60 and 2.65g/cm³. The values measured ex situ vary from 2.427 to 2.68g/cm² and depend on the humidity.⁴⁵ The implication is that the presence of water may cause a swelling of the particles, resulting in a lowering of the density. By this reasoning the conclusion must be that the appropriate density for particles immersed in water should be the lower value, i.e. 2.427g/cm². Acoustic velocity measurements at appropriate frequencies would provide a good method for determining this quantity were it not for the many other parameters about which there is also uncertainty.

The choice of particle size also must be given some consideration. It has been customary to use the Stokes radius. Particle size distributions are generally available as distributions of Stokes radii. In determining this from sedimentation experiments, it is necessary to assume a value of density, although frequently the density value assumed, reported in the literature, is not given. Insofar as both the Stokes radius and the propagation of sound involves the motion of particles through liquid, the Stokes radius should provide a reasonable parameter describing the particle size, provided the same density is used in treating both sets of data. Electron micrographs have indicated particle size considerably smaller for the same clay samples than the Stokes radius determination.⁴⁶ It must here be noted that deflocculation is in general not complete, and it may well be that the so-called deflocculated samples consist

of large numbers of particles that are, in fact, flocs of perhaps 2 or 3 individual platelets.

The effect of particle size is mainly through influencing the relative motion of the particles; small particles following the liquid more closely than large particles. If large flocs are present, they contribute to attenuation through scattering also.

It has been found in the course of this work that both the velocity and absorption cannot be explained by an appropriate choice of these parameters and, hence, on just the basis of ordinary compressibility and relative motion loss considerations. A further influence that now comes into consideration is interparticle forces. In this case the forces, or more appropriately, the derivative of the force with interparticle distance, is expected to vary with concentration as discussed earlier. The relationship is bound to depend on the geometric configuration of the platelets, and this in turn is also likely to undergo statistical alteration with concentration. In other words, the interparticle distances are not likely to vary in a simple way with concentration. The approach taken here is to find empirically the value of the parameter Y needed to bring theory into match with the velocity measurements at each concentration, and then to see if the same values of Y bring agreement for the absorption measurements. It was found that the Y values shown in Fig. 12 bring agreement for both the absorption measurements at 1 MHz (Fig. 13a) and the velocity measurements at 2 MHz (Fig. 11) for which the data are available. Using the same Y values did not meet with this degree of success for the absorption data at

at 5 MHz (see Fig.13b). This set of calculations was done assuming a density of 2.65g/cm^2 and particle size (Stokes diameter) of $1\ \mu$ approximately. Assuming other values for these two parameters would lead to other values of Y but not to better agreement at 5 MHz. The Y values given here are probably maximum values. Choosing a density of 2.427g/cm^2 would reduce the estimate for Y by about 30%.

The numerical Y values can be calculated by using theoretically derived force constants, given in section II, for the relevant type of interaction and assumed geometry. On the assumption that particles are completely deflocculated and assuming uniformly negatively charged plate, the structure of the dispersion is determined by the face-face interaction. The particle separation and spacing depends on the arrangement of the particles. For simplicity, it is assumed that the particles lie in parallel plates, partially filling the plate volume.

The calculation of the particle spacing d or the interfacial spacing for parallel plates H_o , however, is not a simple problem. Limited domains of parallel stacking with face-to-face interaction exist in the suspension, but these domains may not completely fill all the volume. Assuming that they do have a high volume fraction packing (close to unity), Barclay et al.²⁵ have set

$$H_o = 2V_L / m\bar{A} \quad (44)$$

where V_L = volume of the liquid in a suspension containing m grams of clay with a specific area of $\bar{A}\ \text{cm}^2$ per gram of clay particles,

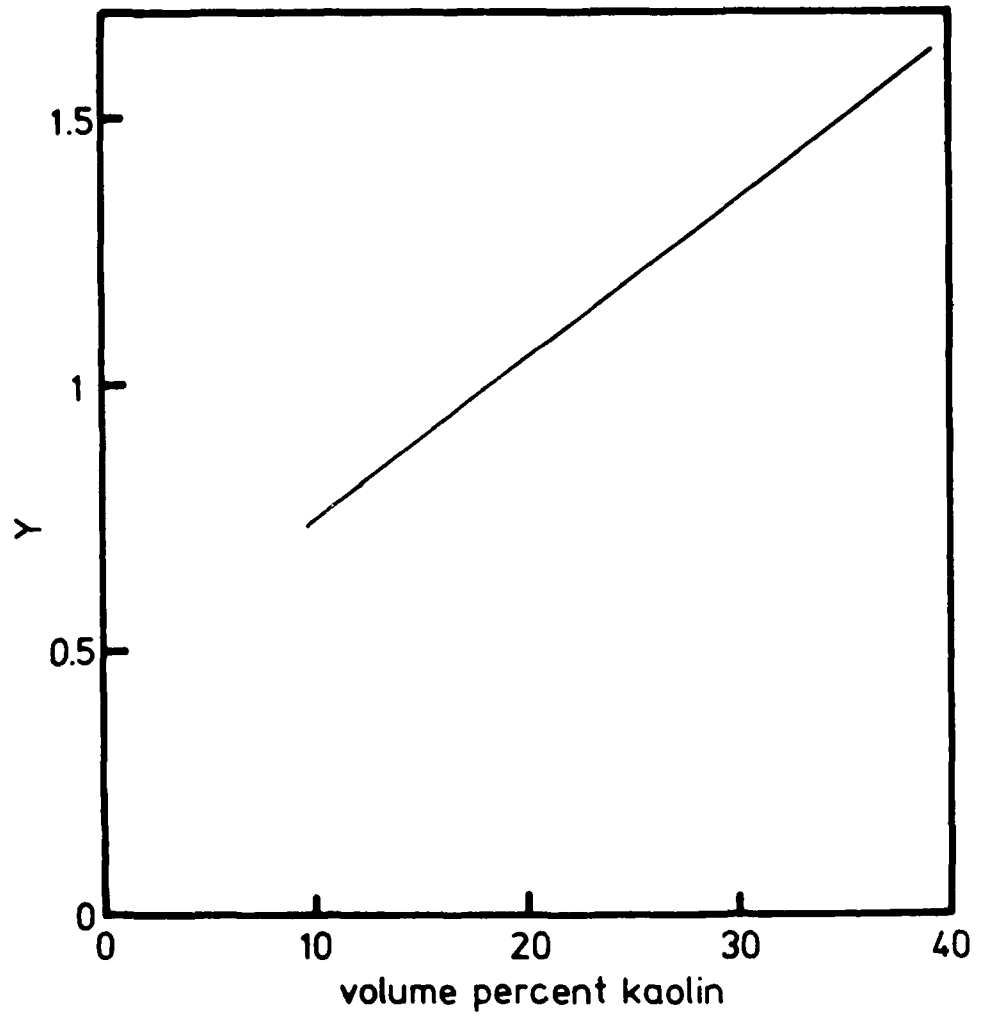


Fig. 12: The Y values for eq. (42) found to bring calculated values of acoustic absorption and velocity into agreement with experimental values at 1 and 2 MHz.

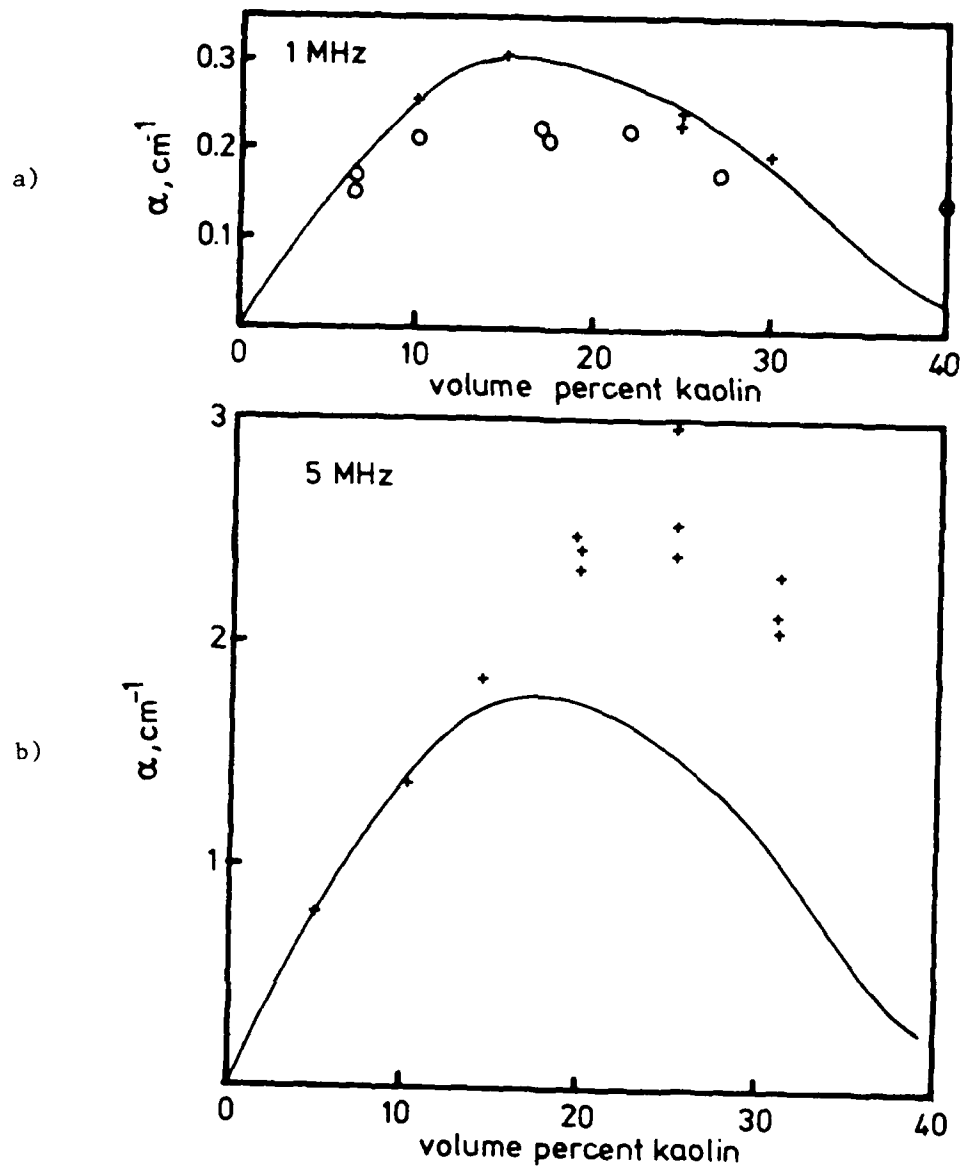


Fig. 13: Experimental and calculated values of acoustic absorption of kaolin suspensions at a) 1 MHz and b) 5 MHz: solid lines are values using Rytov's formula with the Y values given in Fig. 12. Experimental points: + = present work; o = Urick¹⁶

assuming that platelets are very thin (ignoring edge areas). From eq. (44), the spacing between the faces H_o can be shown to be

$$H_o = \left(\frac{1-\phi}{\phi}\right)t \quad (45)$$

where t = thickness of the platelets.

Assuming $y_o=1$, which corresponds to $\psi_o = 25$ mV for 10^{-4} M 1:1 electrolyte concentration, the force constant was calculated using eq. (41); and then the Y values, given in Table II, have been calculated using eq. (42).

TABLE II

Calculated Values of Force Constant f and Y
for Various Volume Fractions ϕ , and Particle Thickness 550\AA

Filled Domains				Half-Filled Domains			
ϕ	$H_o(\text{\AA})$	f dynes cm^2	Y	ϕ	$H_o(\text{\AA})$	f dynes cm^2	Y
.1	4950	4.74×10^5	1.16×10^{-8}	.1	2200	4.36×10^7	2.67×10^{-7}
.2	2200	4.36×10^7	2.67×10^{-7}	.2	825	5.10×10^8	7.80×10^{-7}
.3	1283	2.05×10^8	5.59×10^{-7}	.3	367	2.34×10^9	1.50×10^{-6}
.4	825	5.10×10^8	7.82×10^{-7}	.4	138	1.60×10^{10}	6.12×10^{-6}

The thickness of the particles are taken to be 550\AA , first assuming the plate volume to be completely filled and then half filled. The relationship of these values with concentration for the latter case is shown in Fig. 14. The theoretical Y values are smaller than those determined empirically by ~~six~~ orders of magnitude and do not show the approximately linear relationship with concentrations

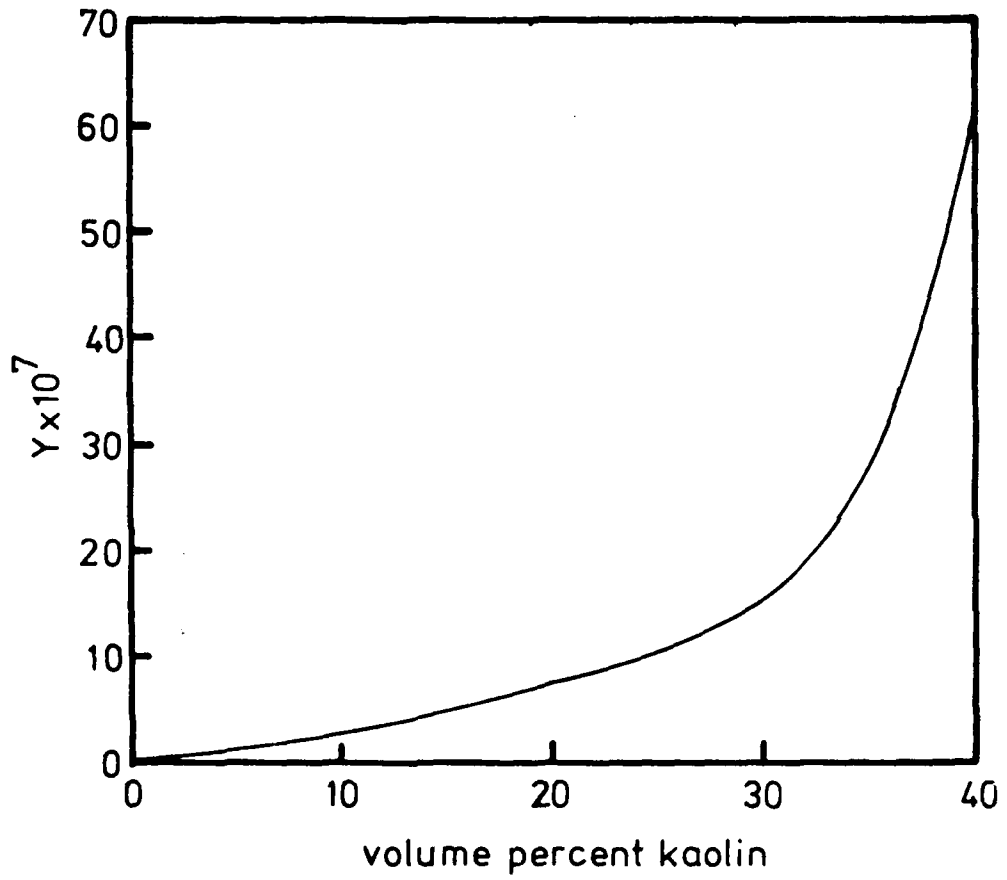


Fig. 14 The Y values calculated as a function of volume % using DLVO theory in a configuration of parallel plates in domains that fill half the volume.

found empirically.

Even though there is a wide discrepancy between the theoretical and experimental values of Y , the reader should keep in mind that the introduction of the factor Y for the particle interactions provides a means for explaining both the velocity and absorption data, provided the Y values are properly adjusted. Further work is required to establish why there is such a large discrepancy in the theoretical and experimental values of Y . It is even possible that there is an intrinsic error in the model or theoretical treatment. It is worth noting that if one assumes the particles occur as small flocs with cardhouse structure, the estimated value of Y are increased by several orders of magnitude although the forces are the same for a given separation. The increase comes through the increase of spacing d , which appears as d^2 in the expression for Y . Further work on the theory is planned.

The proposed theory in Section IV for the effect of the interparticle forces on the velocity and absorption of sound in the deflocculated dispersions predicts an increase in the restoring forces and decrease in the relative motion of particle to liquid which, in turn, leads to a decrease in the absorption and decrease in the velocity. For velocity this case is illustrated in Fig. 11. The best way to demonstrate the influence of the interparticle forces would be to vary these forces by varying the double layer thickness. In the present work double layer thicknesses were not changed. This work is in progress and will be reported shortly.

If one measures the velocity of sound in a dispersion of particles of density similar to the suspending medium, Woods formula (eq. 25) should be appropriate. This is the case with polystyrene latex particles in water. The polystyrene latices show densities from 1.037 to 1.055g/cm³, depending on the preparation.⁴⁷ Velocity measurements at 2 MHz on such polystyrene latex dispersions* in water as a function of volume fraction are given in Fig. 15. The experimental results fit Woods formula if the compressibility is taken as 2.6×10^{-11} and the density 1.047g/cm³. This compressibility value may be compared with that found by Wada⁴⁸ (3.3×10^{-11} for polymethylmetaacrylate particles).

The experimental points deviate from the theoretical curve at concentrations above 20%. Most of the experimental points represent two sets of measurements which could not be distinguished in the figure. The deviation could not be explained with the existing theories. Further work on this matter is in progress.

In the published work on the flocculated kaolin and sediments, the of "frame bulk modulus" has been used to explain the velocity measurements. However, no attempt has been made to describe the nature of the forces responsible. Heterodeflocculation of the kaolin dispersion in neutral pH with montmorillonite gels demonstrated

*The polystyrene latex (styrene-sodium styrene sulphonate polymer) was prepared and ion exchanged by Mr. Y. Chonde. Sodium styrene sulphonate was used as an ionic co-monomer. The particles were a monodispersion with a mean diameter of 1415 Å.

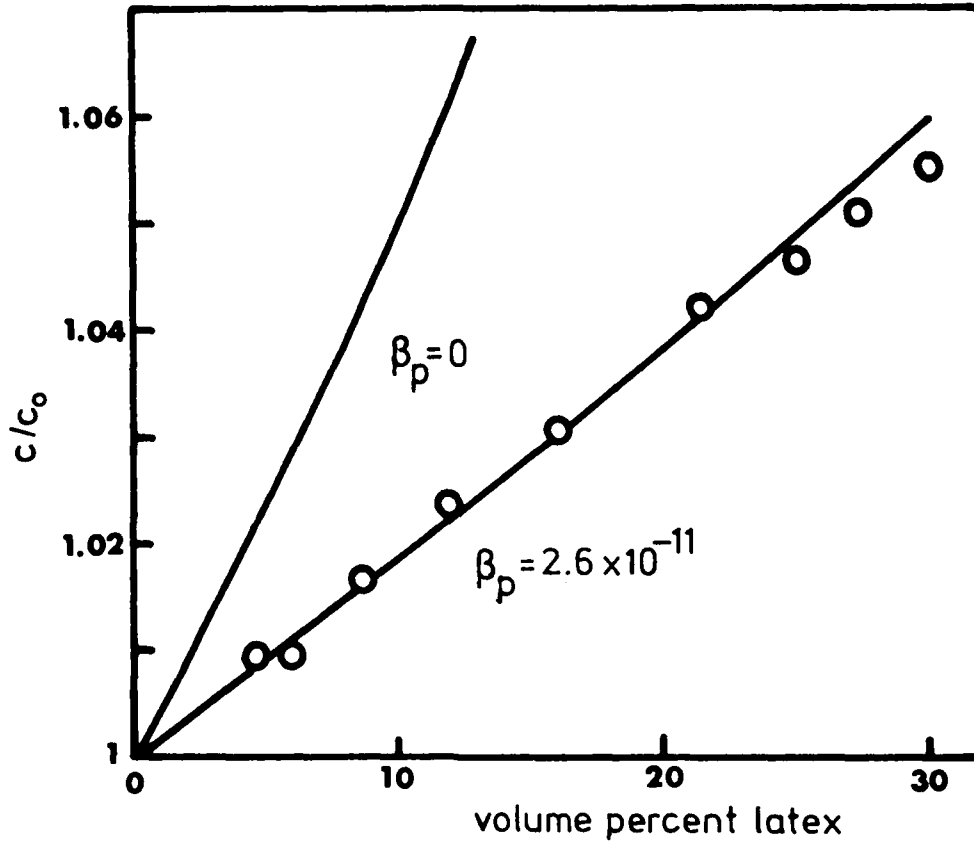


Fig. 15: Ratio of velocity of sound in polystyrene latex suspensions, c , to that in water, c_0 , at 2 MHz. Solid lines are calculated values using Woods Eq. (22) for two values of compressibility β .

the fact that the forces causing the cardhouse structure of "frame bulk modulus" are electrostatic in origin.

Heterodefloculation of kaolin dispersions with montmorillonite gel is shown in Fig. 16. The velocity ratio stays constant (almost) as montmorillonite concentration increases up 0.16 wt.%. At this point a sharp decrease of the velocity ratio to the value of pH deflocculated dispersion. A possible model used in the explanation of this experiment is given in Fig. 16. At neutral pH the dispersion is flocculated and its structure possibly closely resembles the configuration illustrated in Fig. 16a. A typical cardhouse structure is formed due to the heteropolar nature of the kaolin crystals. When montmorillonite particles are introduced into the clay dispersion, they will be attracted by positively charged edges of the kaolin particles. When montmorillonite particles totally cover the edges, deflocculation of the kaolin dispersion is observed.

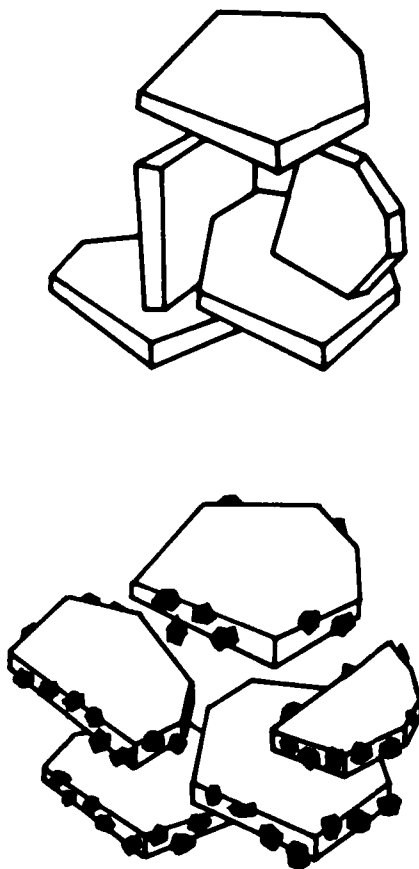


Fig. 16: Possible model for heterodeflocculation of kaolin platelets around neutral pH by specific adsorption of the negatively charged montmorillonite particles on the positively charged edges of kaolin.
A - before deflocculation, showing cardhouse structure
B - deflocculation by adsorption of montmorillonite particles.

Key to Symbols

A	Hamaker constant	V_A	attractive energy
\underline{A}	area in eq. (44)	V_R^ψ	repulsive energy at constant potential
a	radius of particle	V_R^σ	repulsive energy at constant charge
c	velocity of sound	v	velocity of particle
c_o	velocity of sound in water	X_n	particle displacement from equilibrium
d	particle spacing	X_L	particle displacement relevant to the fluid
e	charge of electron	X_u	fluid displacement
F	force	Y	additional term due to interparticle forces
f	force constant	y_o	surface potential
H_o	separation of surfaces	y_m	potential midway between two plates
K_L	bulk modulus of liquid	z	valence
K_P	bulk modulus of particles	α	adsorption coefficient
k	Boltzmann constant	β_L	compressibility of the liquid
\underline{k}	wave number	β_P	compressibility of the particles
m_L	mass of liquid displaced by particles	δ	density of particle
m_P	mass of particles	ϵ	dielectric constant
P	constant in eq. (35)	θ	phase
p	pressure	κ	Debye-Hückel reciprocal length
R	constant in eq. (33)	λ	wavelength
S	frictional drag force		
T	temperature		
U	v-u		
u	velocity of medium		

Key to Symbols (cont.)

μ	kinematic viscosity
ξ	$\omega a^2 / 2\mu$
ρ	density of medium
ρ_0	equilibrium density
ρ_1	deviation from density
σ	ratio of densities of particles to liquid
τ	restoring force
ϕ	volume fraction
ψ	potential
$\psi_{H_0/2}$	potential at midpoint between two surfaces
ω	angular frequency

REFERENCES

1. G. K. Reid, "Ecology of Inland Waters and Estuaries", Reinhold, New York (1961).
2. P. R. Ogushwitz and R. D. Stoll, J. Acoust. Soc. Amer., 65 Suppl. No. 1, S141 (1979); R. D. Stoll and G. M. Bryan, *ibid.*, 47, 1440 (1970).
3. E. L. Hamilton, J. Geophys. Res., 76, 579 (1971); Geophysics, 37, 620 (1972); J. Sedimentary Petrology, 46, 280 (1976).
4. G. Shumway, Geophysics, 25, 451 (1960); *ibid.*, 25, 659 (1960).
5. F. Gassmann, Vierteljahrsschr. Naturforsch. Ges. Zurich, 96, 1 (1951).
6. C. McCann, Acustica, 22, 352 (1969/70).
7. M. A. Barrett-Gültepe, D. H. Everett and M. E. Gültepe, Proc. Inst. Acoust. (London), Vol. 5 (1977).
8. H. Van Olphen, "An Introduction to Clay Colloid Chemistry", Interscience Publishers, New York (1963).
9. I. C. Callaghan and R. H. Ottewill, Disc. Faraday Soc., 57, 110 (1974).
10. R. K. Schofield and H. R. Samson, Disc. Faraday Soc., 18, 135 (1954).
11. P. J. Wangersky, American Scientist, 53, 358 (1965).
12. T. W. Healy, "Selective Adsorption of Organics on Inorganic Surfaces", Chap. 9, p. 187 in Organic Compounds in Aquatic Environments, S. J. Faust and U. V. Hunter, eds., Marcel Dekker, Inc., New York (1971).

13. E. G. Lotse, *Environ. Sci. Tech.*, 2, 353 (1968).
14. A. Weiss, *Anew. Chem.*, 2, 134 (1963).
15. E. J. W. Verwey and J. Th-G. Overbeek, "Theory of the Stability of Lyophobic Colloids", Elsevier, Amsterdam (1948).
16. H. C. Hamaker, *Physica*, 4, 1058 (1937).
17. F. M. Fowkes, *Ind. Eng. Chem.*, 56, 40 (1964).
18. R. Hogg, T. W. Healy and D. W. Fuerstenau, *Trans. Faraday Soc.*, 62, 1638 (1966).
19. G. R. Wiese and T. W. Healy, *Trans. Faraday Soc.*, 66, 490 (1970).
20. G. Frens, Thesis (Utrecht, 1968); G. Frens and J. Th. G. Overbeek, *J. Colloid Interface. Sci.*, 38, 376 (1972).
21. J. P. Friend and R. J. Hunter, *J. Colloid Interface Sci.*, 37, 548 (1971).
22. L. A. Spillman and P. M. Cukor, *J. Colloid and Interface Sci.*, 43, 51 (1973).
23. B. Vincent, C. A. Young and T. F. Tadros, *Faraday Discussions*, No. 65 "Colloidal Stability", (1978), p. 296.
24. A. W. Flegmann, J. W. Goodwin and R. H. Ottewill, *Proc. Brit. Ceramic Soc.*, 13, 31 (1969).
25. L. Barclay, A. Harrington and R. H. Ottewill, *Kolloid-Z. u. Z. Polymere*, 250, 655 (1972).
26. V. S. Nesterov, *Soviet Physics-Acoustics (New York)*, 5(3), 344 (1960).
27. W. S. Ament, *J. Acoust. Soc. Amer.*, 25, 638 (1953).
28. J. R. Allegra and S. A. Hawley, *J. Acoust. Soc. Amer.*, 51, 1545 (1971).

29. P. S. Epstein and R. R. Carhart, *J. Acoust. Soc. Amer.*, 25, 553 (1953).
30. M. C. Davies, *J. Acoust. Soc. Amer.*, 65, 387 (1979).
31. S. M. Rytov, et al., *Zh. Eksperim. i. Teor. Fiz. (USSR)*, 8, 614 (1938).
32. M. E. Gültepe, *Acustica*, 29, 357 (1973).
33. H. Lamb, "Hydrodynamics", 6th ed., Cambridge University Press, Cambridge (1932), p. 657.
34. R. J. Urick, *J. Acoust. Soc. Amer.*, 20, 225 (1948); *ibid.*, 20, 283 (1948).
35. G. G. Stokes, *Cambridge Phil. Soc. Trans.*, 9, 8 (1850); *Mathematical and Physical Papers*", Cambridge University Press, Vol. III, (1922), p. 34.
36. W. König, *Ann. d. Phys. und Chem.*, 42, 353 (1891).
37. A. B. Wood, "A Textbook of Sound", G. Bell and Sons, London (1941).
38. E. L. Hamilton, *J. Geophys. Res.*, 76, 579 (1971).
39. R. J. Urick and W. S. Ament, *J. Acoust. Soc. Amer.*, 21, 115 (1949).
40. L. D. Hampton, *J. Acoust. Soc. Amer.*, 42, 882 (1967).
41. C. Kittel, "Introduction to Solid State Physics", Wiley, (1953).
42. M. Greenspan and C. E. Tscheigg, *J. Res. National Bureau Standards*, Vol. 59, p. 249, No. 4, Oct. 1957, Research paper 2795.

43. L. G. Jackopin and E. Yeager, ONR Technical Report No. 35 (1969).
44. A. Mathieu-Sicaud and G. Levauvasseur, *Compt. Rend.*, 228, 393 (1949); Kruglitskii et al., *Dokl. Akad. Nauk. SSSR*, 159(6), 1367 (1964); N. N. Kruglitskii and V. V. Simurov, *Ukr. Khim. Zh.*, 30(8), 823 (1964).
45. R. E. Grim, "Clay Minerology", McGraw-Hill, New York (1968).
46. J. W. Goodwin, Ph.D. Thesis, Univ. of Bristol (1972).
47. M. E. Gültepe, Ph.D. Thesis, Univ. of Bristol (1979).
48. Y. Wada, H. Hirose, H. Umebayashi and M. Otomo, *J. Phys. Soc. Japan*, 15, 2324 (1960).
49. J. Gregory, *J. Chem. Soc., Faraday Trans. II*, 69, 1723 (1973).
50. M. J. Garvey, Th. F. Tadros and B. Vincent, *J. Colloid Interface Sci.*, 55, 440 (1976).

TECHNICAL REPORT DISTRIBUTION LIST

CASE WESTERN RESERVE UNIVERSITY

Contract N00014-75-C-0557

Project NR 384-305

Director Defense Advanced Research Projects Agency Attn: Technical Library 1400 Wilson Blvd. Arlington, Virginia 22209	3 copies
Office of Naval Research Physics Program Office (Code 421) 800 North Quincy Street Arlington, Virginia 22217	3 copies
Office of Naval Research Assistant Chief for Technology (Code 200) 800 North Quincy Street Arlington, Virginia 22217	1 copy
Naval Research Laboratory Department of the Navy Attn: Technical Library Washington, D.C. 20375	3 copies
Office of the Director of Defense Research and Engineering Information Office Library Branch The Pentagon Washington, D.C. 20301	3 copies
U. S. Army Research Office Box 12211 Research Triangle Park North Carolina 27709	2 copies
Defense Documentation Center Cameron Station (TC) Alexandria, Virginia 22314	12 copies
Director, National Bureau of Standards Attn: Technical Library Washington, D.C. 20234	1 copy
Commanding Officer Office of Naval Research Branch Office 536 South Clark Street Chicago, Illinois 60605	3 copies
Commanding Officer Office of Naval Research Branch Office 1030 East Green Street Pasadena, California 91101	3 copies

San Francisco Area Office Office of Naval Research One Hallidie Plaza Suite 601 San Francisco, California 94102	3 copies
Commanding Officer Office of Naval Research Branch Office 666 Summer Street Boston, Massachusetts 02210	3 copies
New York Area Office Office of Naval Research 715 Broadway, 5th Floor New York, New York 10003	1 copy
Director U. S. Army Engineering Research and Development Laboratories Attn: Technical Documents Center Fort Belvoir, Virginia 22060	1 copy
ODDR&E Advisory Group on Electron Devices 201 Varick Street New York, New York 10014	3 copies
Air Force Office of Scientific Research Department of the Air Force Bolling AFB, D.C. 22209	1 copy
Air Force Weapons Laboratory Technical Library Kirtland Air Force Base Albuquerque, New Mexico 87117	1 copy
Air Force Avionics Laboratory Air Force Systems Command Technical Library Wright-Patterson Air Force Base Dayton, Ohio 45433	1 copy
Lawrence Livermore Laboratory Attn: Dr. W. F. Krupke University of California P. O. Box 808 Livermore, California 94550	1 copy
Harry Diamond Laboratories Technical Library 2800 Powder Mill Road Adelphi, Maryland 20783	1 copy

Naval Air Development Center Attn: Technical Library Johnsville Warminster, Pennsylvania 18974	1 copy
Naval Weapons Center Technical Library (Code 753) China Lake, California 93555	1 copy
Naval Training Equipment Center Technical Library Orlando, Florida 32813	1 copy
Naval Underwater Systems Center Technical Library New London, Connecticut 06320	1 copy
Commandant of the Marine Corps Scientific Advisor (Code RD-1) Washington, D. C. 20380	1 copy
Naval Ordnance Station Technical Library Indian Head, Maryland 20640	1 copy
Naval Postgraduate School Technical Library (Code 0212) Monterey, California 93940	1 copy
Naval Missile Center Technical Library (Code 5632.2) Point Mugu, California 93010	1 copy
Naval Ordnance Station Technical Library Louisville, Kentucky 40214	1 copy
Commanding Officer Naval Ocean Research & Development Activity Technical Library NSTL Station, Mississippi 39529	1 copy
Naval Explosive Ordnance Disposal Facility Technical Library Indian Head, Maryland 20640	1 copy
Naval Ocean Systems Center Technical Library San Diego, California 92152	1 copy
Naval Surface Weapons Center Technical Library Dahlgren, Virginia 22448	1 copy

Naval Surface Weapons Center (White Oak) Technical Library Silver Spring, Maryland 20910	1 copy
Naval Ship Research and Development Center Central Library (Code L42 and L43) Bethesda, Maryland 20084	1 copy
Naval Avionics Facility Technical Library Indianapolis, Indiana 46218	1 copy